

Master's Thesis

Title

**Self-Organizing Clustering Method
for Energy-Efficient Data Gathering in Sensor Networks**

Supervisor

Professor Masayuki Murata

Author

Junpei Kamimura

February 15th, 2005

Department of Information Networking
Graduate School of Information Science and Technology
Osaka University

Abstract

By deploying wireless sensor nodes and composing a sensor network, one can remotely obtain information about the behavior, conditions, and positions of entities in a region. Since sensor nodes operate on batteries, energy-efficient mechanisms for gathering sensor data are indispensable to prolong the lifetime of a sensor network as long as possible. A sensor node consumes energy in observing its surroundings, transmitting data, and receiving data. Especially, energy consumption in data transmission scales proportionally to the n -th power of the radius of the radio signal. Therefore, cluster-based data gathering mechanisms effectively save energy. In cluster-based data gathering, since each node can save transmission power and the number of collisions is also reduced, sensor networks can live for longer period. In clustering, however, we need to consider that a cluster-head consumes more energy than the other nodes in receiving data from cluster members, fusing data to reduce the size, and sending the aggregated data to a base station.

In this study, first, we propose a novel clustering method where energy-efficient clusters are organized in a distributed way through local communication among neighboring sensor nodes. Our clustering method is based on the idea of ANTCLUST, a clustering algorithm which applies a colonial closure model of ants. We adopt multihop transmission among cluster-heads taking into account a limitation on the radio transmission range. Second, we analyze the relationship among the radius of a cluster, the amount of energy consumed in data gathering, and the distance of a cluster-head to the base station, for a cluster-head to autonomously determine its cluster radius to prolong the lifetime of a sensor network. Through simulation experiments, we verified that our method can gather sensor data with less energy consumption than methods with a fixed radius by more than the half at most. In addition, we also showed that our method was adaptive to changes of network conditions when the maximum transmission range was large.

Keywords

Sensor Network, Data Gathering, Clustering, Biological System

Contents

1	Introduction	6
2	Sensor Network	9
3	ANTCLUST: Ant-based Clustering Algorithm	10
4	Self-Organizing Clustering Method	13
4.1	Overview	13
4.2	Cluster-Head Candidacy Phase	15
4.3	Cluster Formation Phase	15
4.4	Registration Phase	17
4.5	Data Transmission Phase	18
5	Analysis of Energy Consumption in Cluster-based Data Gathering	18
5.1	Energy Consumption Model in Cluster-Based Data Gathering	19
5.2	Derivation of $E_{all_m \rightarrow h}$	23
5.3	Derivation of E_{head1}	38
5.4	Derivation of E_{head2}	38
5.5	Derivation of E_{head3}	39
5.6	Results of the Analysis	39
6	Simulation Experiments	41
7	Conclusion	43
	References	46
	Acknowledgements	46

List of Figures

1	Sensor network	6
2	Overview of our proposal	13
3	An example where $(head_i \neq head_j) \wedge (Acceptance(i, j) = True)$	16
4	Model of sensor network for analysis	20
5	Overlapping clusters	21
6	Region covered by one cluster	22
7	Region S that a cluster-head is responsible for	22
8	Three conditions among the cover region and the monitoring region	23
9	Cases of intra-cluster transmissions	25
10	Cases of intra-cluster transmissions	26
11	Transition of $E_{cluster}$ ($W = 100$)	47
12	Transition of E_{node} ($W = 100$)	47
13	Transition of $E_{cluster}$ ($W = 200$)	48
14	Transition of E_{node} ($W = 200$)	48
15	Transition of $E_{cluster}$ ($W = 400$)	49
16	Transition of E_{node} ($W = 400$)	49
17	Transition of r_{opt} ($W = 100$)	50
18	Transition of r_{opt} ($W = 200$)	50
19	Transition of r_{opt} ($W = 400$)	51
20	Cumulative amount of received data and total amount of consumed energy ($W =$ 100)	52
21	Cumulative amount of received data and total amount of consumed energy ($W =$ 200)	53
22	Cumulative amount of received data and total amount of consumed energy ($W =$ 400)	54

List of Tables

1	Status information of sensor node	14
2	Parameters used in analysis	21

1 Introduction

With recent advancements and developments in Micro Electro Mechanical System (MEMS) technologies, large-scale networks of integrated wireless sensor nodes have become available. A sensor node is very compact, containing one or more sensors, computation and radio communication capabilities, and a power supply. By deploying sensor nodes and composing a sensor network, one can remotely obtain information about behavior, conditions, and the position of entities in a region [1]. Typically, a sensor network consists of many sensor nodes and a base station as illustrated in Fig. 1. Hundreds or thousands of wireless sensor nodes are distributed in a region in uncontrolled and unorganized ways. Sensor data obtained at sensor nodes are sent to a base station through wireless communication, then presented to a user or sent to a remote host.

Since sensor nodes derive power from batteries, an energy-efficient data gathering mechanism is indispensable to observe the region as long as possible. A sensor node consumes its energy in monitoring its environment and receiving or sending radio signals. The amount of energy consumed in radio transmission scales proportionally to the k -th power of the range of the radio signal propagation [2, 3]. Since the distance from sensor nodes to the base station is larger than among neighboring sensor nodes, it is energy-inefficient for all sensor nodes to send their data directly to a distant base station. Consequently, cluster-based data gathering mechanisms are proposed to effectively save energy [2-5]. In cluster-based mechanisms, groups of neighboring sensor nodes form clusters. In each cluster, one representative node called a cluster-head gathers sensor data from its members and sends the collected data to the base station.

Since cluster-heads consume more energy than cluster members in receiving sensor data from their members, the processing received data, and sending the aggregated data to the base station,

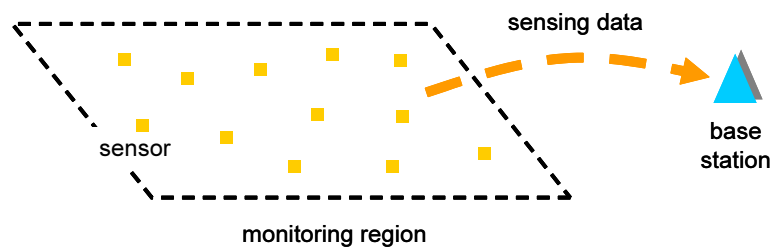


Figure 1: Sensor network

the role of the cluster-head must be rotated among sensor nodes. For example, in LEACH [3], one of the most popular clustering protocols, a pre-determined percentage of sensor nodes become cluster-heads. They first advertise their candidacy to the rest of the sensor nodes. Hearing advertisements, each sensor node chooses the closest cluster-head and registers itself as a cluster member. Eventually clusters are formed. Cluster members send their sensor data to a cluster-head. Then each cluster-head combines all n -bit data into a single n -bit data message and sends it to the base station. By defining the probability of candidacy such that a sensor node which has not become a cluster-head recently is more likely to advertise its candidacy, LEACH rotates the role of cluster-heads among the sensor nodes. HEED [5] takes into account residual energy of sensor nodes in electing cluster-heads. The probability CH_{prob} of candidacy is given by multiplying the pre-determined constant probability and the percentage of residual energy against the maximum capacity. Each sensor node advertises its candidacy within a certain range with probability of CH_{prob} and then doubles its own CH_{prob} . Sensor nodes which received candidacy choose the cluster-head with the minimum cost.

There are several requirements for a clustering method. First, a clustering method should be completely distributed because central control of hundreds or thousands of sensor nodes is not feasible. Second, clusters are needed to be geographically well-distributed for well-balanced energy consumption among sensor nodes. Third, of course, a clustering method itself should be energy-efficient. Fourth, since sensor nodes are dynamically deployed, moved, and halted, a clustering method should be able to adapt to changes of the sensor network. Earlier examples, LEACH and HEED do not necessarily satisfy all requirements. Moreover, LEACH only satisfies the third point and falls into the category of distributed mechanisms. However, LEACH's clustering algorithm assumes that sensor nodes are homogeneous and equal. In reality, however, their battery capacities are different. In addition, the amount of energy consumed in gathering data also differs among cluster-heads, depending on the number of cluster members and their positions in the region. Energy consumption also differs among cluster members due to the difference in the distance to a cluster-head. Some sensor nodes might also be deployed later for denser observations. Consequently, the residual energy is not necessarily equal among all sensor nodes. In addition, the optimum percentage of cluster-heads has to be determined in advance, considering the topology of the sensor network. Therefore, LEACH cannot adapt to such changes in sensor networks as addition, removal, and transfer of sensor nodes, however the percentage of cluster-heads considerably

affects the efficiency of data gathering. Finally, for organized clusters to cover an entire sensor network, each cluster-head must broadcast its own advertisement to all the other nodes, another inefficient use of energy. To tackle the problem, some variations of LEACH are proposed in [3]. LEACH-C (LEACH-centralized) is a centralized protocol, which takes into account the residual energy in choosing sensor nodes for cluster-heads. HEED also takes into account the residual energy of the sensor nodes in electing cluster-heads, but it needs multiple broadcasting to form clusters and consumes more energy. Our goal is to propose a new clustering method to satisfy the above mentioned features, where sensor nodes autonomously form appropriate clusters through local communication among neighboring sensor nodes.

In biology, ants and other social insects construct clusters, i.e., colonies, parties, and cemeteries in self-organizing ways [6]. For example, ants recognize each other by exchanging a chemical substance. If they are similar, the ant is welcomed and treated as a member of the same nest. Taking inspiration from such biological systems, much research has been done in the fields of data clustering and graph partitioning [7, 8]. In [7], ANTCLUST is proposed, which is an algorithm based on an ant behavior model of colonial closure, to solve data clustering problems. In ANTCLUST, two randomly chosen objects meet. Based on their similarity, a cluster is created, merged, or deleted. By repeating meetings, an appropriate set of clusters is eventually formed so that similar objects are accommodated in the same cluster.

In this study, based on ANTCLUST, we propose a novel clustering method that organizes energy-efficient clusters through local interactions among sensor nodes. Basically, our method presented in this thesis is based on our previous research work [9], which was verified to outperform LEACH and HEED in terms of the lifetime of sensor networks and the amount of data gathered. We newly consider multihop communications among cluster-heads taking into account the limitation in the transmission range of radio signals. In our method, sensor nodes with more residual energy independently become cluster-heads. Sensor nodes meet through local radio communications and find other clusters. Each sensor node with less residual energy chooses a cluster based on the residual energy of the cluster-head, distance to the cluster-head, and an estimation of the cluster size. Energy-efficient clusters are eventually formed that extend the life of the sensor network. Each cluster-head gathers sensor data from its members and sends it to a base station by forwarding it over intermediate cluster-heads, i.e., multihop transmission. In the multihop transmission among cluster-heads, a cluster-head additionally consumes energy in relaying sen-

sensor data from more distant clusters. To have energy-efficient clusters, the radius of each cluster must be carefully determined. As the radius of the cluster increases, the amount of sensor data a cluster-head must gather in its members and send to the next-hop cluster-head increases, whereas the frequency of becoming a cluster-head becomes smaller. In addition, the amount of sensor data that a cluster-head must relay depends on the distance from the base station. We analytically investigate the relationship among the cluster radius, the amount of energy consumed, and the distance of a cluster-head to the base station. Based on the analytical results, each cluster-head can independently determine its cluster radius that leads to energy-efficient cluster-based data gathering.

The rest of the thesis is organized as follows. Section 2 explains assumptions of sensor networks considered in this thesis. Section 3 introduces ANTCLUST, a clustering algorithm on which our method is based. Then in Section 4, we propose a new clustering method for energy-efficient data gathering in sensor networks. In Section 5, we analytically derive the appropriate cluster radius that minimizes the amount of energy consumed in data gathering. We evaluate our self-organizing clustering method in Section 6. Finally, Section 7 concludes the thesis and describes future research issues.

2 Sensor Network

We consider an application of field monitoring where sensor data are gathered from all sensor nodes to a base station at regular intervals and/or on demand. Examples of applications include habitat monitoring, agriculture, and patrols of environments [1].

Sensor networks can contain hundreds or thousands of sensor nodes. To avoid installation cost and the need for careful planning, sensor nodes are deployed in the region to monitor in an uncontrolled and unorganized way. Since sensor nodes operate on energy-limited and irreplaceable batteries. The capacity of batteries can differ among sensor nodes. Sensor nodes stop due to starvation of battery power, move from one place to another, and are deployed at different times. Sensor nodes can determine the distance to other sensor nodes and the base station from the received signal strength or their positions obtained by using Global Positioning System (GPS) or another position detection mechanism [10]. Sensor nodes have a wireless transmitter and receiver. The range of the radio signals can be adjusted depending on the distance to the receiver within the maximum transmission range. Control phases, e.g, cluster formation phase, are synchronized

among all sensor nodes. Although other clustering methods or cluster-based data gathering methods such as LEACH make similar or even stronger assumptions, we should note here that the number of applications where these assumptions hold would be limited.

3 ANTCLUST: Ant-based Clustering Algorithm

Ants synthesize a chemical substance called colony odor which differs by individuals, species, and environment; they spread it on their cuticles [11, 12]. When two ants meet, they recognize whether they belong to the same nest by exchanging and comparing these chemical substances, which is updated at each meeting. After spending some time in the nest and repeatedly meeting other ants, a young ant can prepare an appropriate chemical substance to recognize its mates.

ANTCLUST is a clustering algorithm which applies a colonial closure model and regards an object as an ant and a cluster as a nest [7]. A similarity $Sim(i, j) \in [0, 1]$ is defined between a pair of objects i and j . Each object i has a cluster identifier, $Label_i$, an acceptance threshold of similarity, $Template_i$, an estimator of the cluster size, $M_i \in [0, 1]$, and an estimator, $M_i^+ \in [0, 1]$, which measures how well the object is accepted in the cluster. They are initialized as $Label_i = 0$, $M = 0$, and $M^+ = 0$. $Template_i$ is defined through a learning phase where object i experiences random meetings.

$$Template_i \leftarrow \frac{\overline{Sim(i, \cdot)} + \max(Sim(i, \cdot))}{2}. \quad (1)$$

$\overline{Sim(x, \cdot)}$ and $\max(Sim(x, \cdot))$ represent the average and the maximum value of similarity between object x and all other objects that object x has met, respectively.

In ANTCLUST, two randomly chosen objects meet. Based on their similarity, threshold values, and clusters, they create, merge, or delete clusters. By repeatedly conducting random meetings, clusters are appropriately organized so that objects in the same cluster become more similar with one another than those in different clusters.

We consider here the case when two objects i and j meet. First, two objects i and j decide whether they accept their counterpart according to the similarity $Sim(i, j)$ and threshold values $Template_i$ and $Template_j$.

$$Acceptance(i, j) \Leftrightarrow (Sim(i, j) > Template_i) \wedge (Sim(i, j) > Template_j). \quad (2)$$

Then $Template_i$ and $Template_j$ are updated by Eq. (1). Next, their $Labels$ are compared. When neither of them belongs to any cluster and they accept each other, a new cluster is created.

$$\begin{aligned}
& Label_i \leftarrow Label_{NEW}, Label_j \leftarrow Label_{NEW}, \\
& \text{if } (Label_i = Label_j = 0) \\
& \quad \wedge (Acceptance(i, j) = True).
\end{aligned} \tag{3}$$

If one of the two objects, say object i , does not belong to any cluster, and if they accept each other, object i joins the cluster of the other.

$$\begin{aligned}
& Label_i \leftarrow Label_j, \\
& \text{if } (Label_i = 0) \\
& \quad \wedge (Label_j \neq 0) \\
& \quad \wedge (Acceptance(i, j) = True).
\end{aligned}$$

When two objects belong to the same cluster and they accept each other, they increase their size estimate of their cluster:

$$\begin{aligned}
& M_i \leftarrow (1 - \alpha)M_i + \alpha, M_j \leftarrow (1 - \alpha)M_j + \alpha, \\
& M_i^+ \leftarrow (1 - \alpha)M_i^+ + \alpha, M_j^+ \leftarrow (1 - \alpha)M_j^+ + \alpha, \\
& \text{if } (Label_i = Label_j) \\
& \quad \wedge (Label_i \neq 0) \\
& \quad \wedge (Label_j \neq 0) \\
& \quad \wedge (Acceptance(i, j) = True).
\end{aligned} \tag{4}$$

Here, α is a constant between 0 and 1. When two objects belong to the same cluster and they

reject each other, they first update the size of their estimates:

$$\begin{aligned}
M_i &\leftarrow (1 - \alpha)M_i + \alpha, \quad M_j \leftarrow (1 - \alpha)M_j + \alpha, \\
M_i^+ &\leftarrow (1 - \alpha)M_i^+, \quad M_j^+ \leftarrow (1 - \alpha)M_j^+, \\
&\text{if } (Label_i = Label_j) \\
&\quad \wedge (Label_i \neq 0) \\
&\quad \wedge (Label_j \neq 0) \\
&\quad \wedge (Acceptance(i, j) = False).
\end{aligned} \tag{5}$$

Here, object x with the smaller estimate loses its cluster.

$$Label_x \leftarrow 0, \quad M_x \leftarrow 0, \quad M_x^+ \leftarrow 0, \tag{6}$$

where $x = \{x | M_x^+ = \min(M_i^+, M_j^+)\}$. When two objects belong to different clusters and they accept each other, they first estimate how the size of their clusters will be changed:

$$\begin{aligned}
M_i &\leftarrow (1 - \alpha)M_i, \quad M_j \leftarrow (1 - \alpha)M_j, \\
&\text{if } (Label_i \neq Label_j) \\
&\quad \wedge (Label_i \neq 0) \\
&\quad \wedge (Label_j \neq 0) \\
&\quad \wedge (Acceptance(i, j) = True).
\end{aligned} \tag{7}$$

Then, object x in the smaller cluster changes its cluster.

$$Label_x \leftarrow Label_{(k | k \in \{i, j\} \setminus \{x\})}, \tag{8}$$

where $x = \{x | M_x = \min(M_i, M_j)\}$. When none of the above conditions holds, nothing happens.

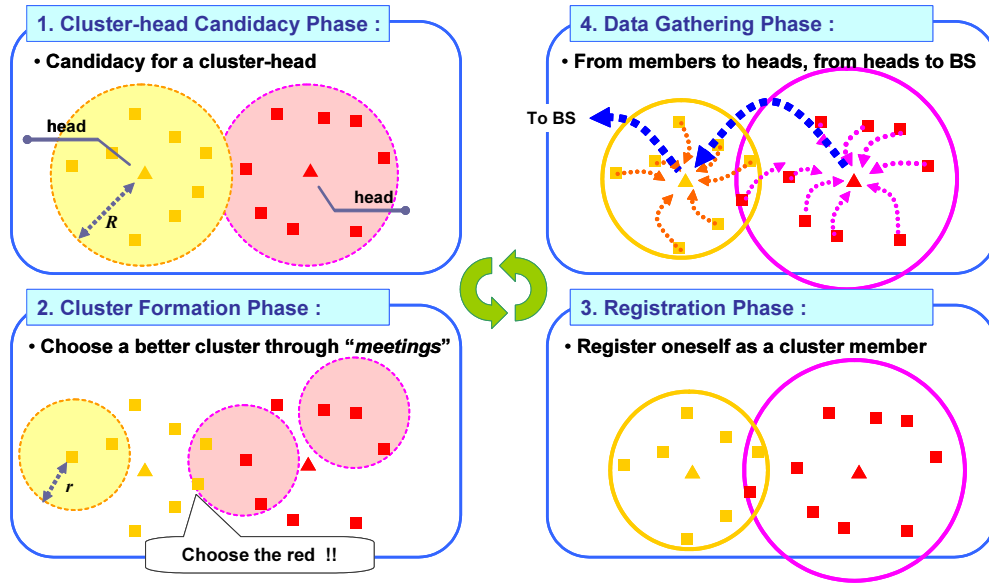


Figure 2: Overview of our proposal

4 Self-Organizing Clustering Method

4.1 Overview

In our method, we regard a sensor node as an ant and a cluster as a nest. The similarity of one sensor node to another corresponds to the distance from the sensor node to each cluster-head. Sensor nodes meet through wireless communications. Since a sensor node usually has an omni-antenna, a radio signal is broadcast, and it is received by all sensor nodes within its transmission range. Thus, it is a one-to-many communication. In addition, it is a one-way communication. In our method, only the receiver of a signal adjusts its cluster while in ANTCLUST both encountered objects adjust their clusters.

A cycle of data gathering, called a round, consists of four phases [3]: (i) cluster-head candidacy, (ii) cluster formation, (iii) registration, and (iv) data transmission as illustrated in Fig. 2. In the cluster-head candidacy phase, all sensor nodes initially consider themselves as candidates for cluster-head. A sensor node with more residual energy has a chance to advertise its candidacy earlier than others. It becomes a cluster-head by broadcasting an advertisement within a limited range R . Those sensor nodes that receive advertisements from other sensor nodes abandon their candidacy and join a cluster. Details of the cluster-head candidacy phase will be given in 4.2.

Table 1: Status information of sensor node

Information about sensor node i	
i	node identifier
e_i	residual energy
c_i	coordinates
$Template_i$	threshold of similarity, initial value R
P_i	probability of candidacy [0, 1], initial value 0.5
Information about a cluster of sensor node i	
$head_i$	identifier of a cluster-head
E_i	residual energy of a cluster-head
C_i	coordinates of a cluster-head
M_i	estimator of the number of cluster members
System parameters	
R	radius for broadcasting candidacy for cluster-head
r	radius for broadcasting cluster information for meetings
P_{ex}	proportion of social sensor nodes that cause meetings [0, 1]

In the cluster formation phase, sensor nodes meet through radio communications. A percentage P_{ex} of sensor nodes that are not cluster-heads broadcast information about their clusters within a limited range r ($r < R$). Each of the neighboring sensor nodes which receive broadcast messages determines which cluster to join based on the information about its own cluster and the newly advertised clusters. Further details will be given in Section 4.3. Next in the registration phase, which will be explained in Section 4.4, each sensor node registers itself as a cluster member by sending a registration message to a cluster-head. In the data transmission phase, cluster members send their data to the cluster-head. The cluster-head receives its members' data and aggregates them into one. Then it sends the aggregated data to a cluster-head which is closer to a base station or directly to a base station. Details of the data transmission phase will be given in Section 4.5. The beginning of each round and the timing of phase-changes are synchronized among sensor nodes.

For constructing clusters, a sensor node maintains the information about itself and its cluster-head as listed in Table 1. Among the parameters in Table 1, the first three are static. $Template_i$ and P_i are initialized when sensor node i is deployed, and they are updated every round. Information about a cluster is initialized at the beginning of each round. The last three parameters are initialized at deployment, but they can be adjusted according to conditions surrounding sensor node i .

4.2 Cluster-Head Candidacy Phase

At the beginning of a round, all sensor nodes consider themselves candidates for cluster-head. Cluster information is initialized as:

$$head_i \leftarrow i, E_i \leftarrow e_i, C_i \leftarrow c_i, M_i \leftarrow 1. \quad (9)$$

Assuming that the cluster-head candidacy phase has a T time unit duration, sensor node i announces its candidacy within the radius of R at $T \times (1 - P_i) + K$, where K is a random value $[0, (Tp - 1)]$ to reduce the possibility of collisions among sensor nodes with identical P_i and weaken the assumption of the synchronization among sensor nodes. To prolong the lifetime of a sensor network, energy consumption among sensor nodes must be balanced. By adjusting P_i in accordance with the residual energy of neighboring sensor nodes as explained in the next subsection, sensor nodes with more residual energy are more likely to become cluster-heads. p is a constant value used in increasing or decreasing P_i in Eq. (13). An advertisement of candidacy contains cluster information, i.e., $head_i, E_i, C_i$, and M_i , and its own residual energy e_i . When a candidacy is announced, E_i is obviously identical to e_i .

When a sensor node that has not yet announced its candidacy receives an advertisement message from another sensor node, it abandons its own candidacy and becomes a member of the cluster. Furthermore, when a sensor node that already belongs to a cluster receives another advertisement message, it considers the offer and conducts the same procedure as in the next cluster formation phase to determine which cluster it should join.

4.3 Cluster Formation Phase

At the end of the cluster-head candidacy phase, every sensor node belongs to a cluster as either a cluster-head or as a member. A percentage P_{ex} of sensor nodes decide to be social and broadcast information about their clusters within a radius of r . On receiving an advertisement, sensor nodes within radio signal range meet other sensor nodes and determine their clusters. The format for a meeting advertisement is the same as for candidacy. If a sensor node is a cluster-head, it does not initiate a meeting. Hereafter we describe a case where sensor node i receives an advertisement from sensor node j .

If sensor node i is not a cluster-head, then it adjusts its cluster. First, sensor node i decides

cluster:

$$\begin{aligned}
& head_i \leftarrow head_j, E_i \leftarrow E_j, C_i \leftarrow C_j, M_i \leftarrow M_j + 1, \\
& \text{if } (head_i \neq head_j) \\
& \wedge (Acceptance(i, j) = True) \\
& \wedge \left(\frac{E_j}{M_j \cdot d^2(i, head_j)} \geq \frac{E_i}{M_i \cdot d^2(i, head_i)} \right).
\end{aligned} \tag{12}$$

Except for the procedure mentioned above, sensor node i does nothing for cluster formation.

Regardless of whether sensor node i is a cluster-head, it updates the probability P_i of its cluster-head candidacy to reflect the relationship among its own residual energy e_i and that of sensor node j , e_j :

$$P_i \leftarrow \begin{cases} \min(1, P_i + p), & \text{if } e_i > e_j \\ \max(0, P_i - p), & \text{if } e_i < e_j \\ P_i, & \text{if } e_i = e_j. \end{cases} \tag{13}$$

Here, p is a constant value which satisfies $p \in [0, 1]$. Thus, the probability of a candidacy is determined in relation to the residual energy of surrounding sensor nodes, not by its absolute amount. Next, sensor node i updates threshold $Template_i$:

$$Template_i = \frac{\overline{d(i, \cdot)} + \max(d(i, \cdot))}{2} \tag{14}$$

where, $\overline{d(i, \cdot)}$ and $\max(d(i, \cdot))$ give the mean and maximum distance between sensor node i and all cluster-heads that sensor node i recognizes through receiving advertisements.

4.4 Registration Phase

Each sensor node registers itself as a cluster member by sending a registration message to a cluster-head. Through the registration phase, a cluster head recognizes its members. In a case that CSMA is used in the following data gathering phase, a cluster-head can estimate the maximum duration needed to gather sensor data from its members by using an analytical model of CSMA communications [13]. If TDMA is employed in the data gathering phase, a cluster-head determines slot assignments. At the end of the registration phase, a cluster-head notifies its members of the sched-

ule. Each cluster member can turn off unused components until its turn comes.

4.5 Data Transmission Phase

At the beginning of the data transmission phase, cluster members send their sensor data to a cluster-head by CSMA, TDMA, or any other MAC protocol. The cluster-head receives sensor data from its members and aggregates them and its own sensor data into one. If data fusion is applicable, the size of the aggregated data becomes much smaller than the sum of sensor data [14]. Then, the aggregated data are sent to the next-hop cluster-head, which is determined by a multihop routing protocol. Many publications deal with energy-efficient routing protocols for sensor networks, e.g., [15]. Since we only focus on an energy-efficient clustering method, a routing protocol is out of scope of this thesis.

We consider here a simple tree-based routing method, which resembles to [16]. First, a base station broadcasts a beacon signal with a limited transmission power. On receiving beacon signals, those sensor nodes within the range of the beacon signals then advertise that they are at the first level of the tree within the range of radio signals. Receiving those advertisements, sensor nodes around can recognize that they are at the second level and they can send their sensor data to the base station via a mediation of the sources of the advertisements. Then, they also broadcast advertisement messages for their level. By repeating advertisement level by level, all sensor nodes determine their levels in the tree and identify their parent nodes. In the data aggregation phase, a cluster-head sends the aggregated sensor data to a cluster-head which is the closest to the base station among its parents.

5 Analysis of Energy Consumption in Cluster-based Data Gathering

To prolong the lifetime of a sensor network, cluster radii must be carefully determined. For example, if a radius is large, a cluster-head consumes much energy in receiving sensor data from its members and sending the aggregated data to the next-hop node. In addition, cluster-members consumes much energy in sending their data to the distant cluster-head. However, at the same time, since the number of nodes in a cluster increases, a sensor node becomes a cluster-head less frequently. On the contrary, if a radius is small, the amount of energy consumed in data gathering becomes small at the sacrifice of frequent rotation of the role of cluster-head. In addition to

intra-cluster communications, the distance to a base station also affects the energy consumption of a cluster. If a cluster is close to a base station, a cluster-head has to relay more sensor data from its outside region in multihop communication among cluster-heads. In this section, for each cluster-head to independently determine an appropriate radius of its cluster, R in our method, we analytically investigate the relationship among the energy consumption, cluster radius, and the distance of a cluster-head to the base station.

5.1 Energy Consumption Model in Cluster-Based Data Gathering

To generalize the problem, we consider energy consumed in gathering data from cluster members to a cluster-head and sending aggregated data to the base station by multihop transmission among cluster-heads. Therefore, since we do not consider how clusters are organized, results in this section can be applied to other cluster-based data gathering methods. We ignore energy consumed in MAC layer processing in carrier sense, collision detection, and retransmission. The energy consumed in transmitting and receiving a k bit message at d m is given in Eqs. (15) through (17) [3].

$$E_{transmit}(k, d) = \begin{cases} k \cdot (E_{elec} + \varepsilon_{fs} \cdot d^2), & \text{if } d < d_0 \\ k \cdot (E_{elec} + \varepsilon_{mp} \cdot d^4), & \text{if } d \geq d_0 \end{cases} \quad (15)$$

$$(16)$$

$$E_{receive}(k) = k \cdot E_{elec} \quad (17)$$

A sensor node consumes E_{elec} (nJ/bit) in transmitter or receiver circuitry and ε (pJ/bit/m $^\alpha$) in transmitter amplifier. The threshold d_0 is introduced to take into account the effect of multi-path fading.

The total energy $E_{cluster}$ consumed in one cluster is given by Eq. (18).

$$E_{cluster} = E_{all_m \rightarrow h} + E_{head1} + E_{head2} + E_{head3} \quad (18)$$

$E_{all_m \rightarrow h}$ corresponds to the total amount of energy consumed by cluster members in sending their sensor data to a cluster-head. E_{head1} is the energy consumed by a cluster-head in receiving sensor data from its members. E_{head2} is the energy consumed by a cluster-head in receiving sensor data

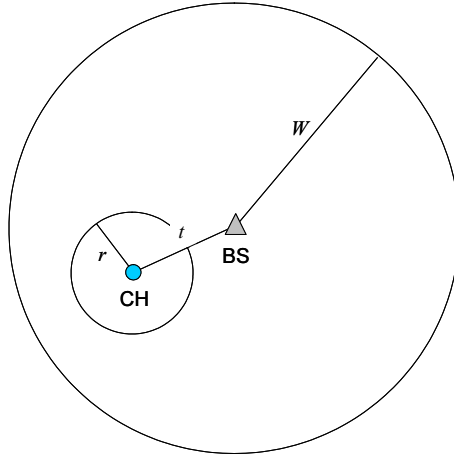


Figure 4: Model of sensor network for analysis

from other cluster-heads which it has to forward toward the base station. Finally, E_{head3} stands for the energy consumed by a cluster-head in sending the aggregated sensor data to the next-hop cluster-head or the base station. The amount of energy consumed per sensor node, E_{node} , averaged over multiple rounds, where the role of cluster-head is rotated, is given by the following equation.

$$E_{node} = \frac{E_{cluster}}{n}, \quad (19)$$

where n denotes the number of sensor nodes in a cluster. When we assume the uniform distribution of sensor nodes, the following equation holds.

$$n = \rho \times S_{cluster}, \quad (20)$$

where ρ is the density of the sensor nodes and $S_{cluster}$ corresponds to the area from which a cluster-head gathers sensor data.

Parameters used in our analysis are summarized in Table 2. In our analysis, we consider a circular monitoring region of radius W at whose center a base station is located as in Fig. 4. We assume that sensor nodes are uniformly distributed in the monitoring region with density ρ . Through simulation experiments of our proposed clustering method, we observed that neighboring clusters overlapped with each other by the half of the region of cluster as shown in Fig. 5. In Fig. 5, a square corresponds to the base station, crosses stand for cluster-heads, and dashed circles

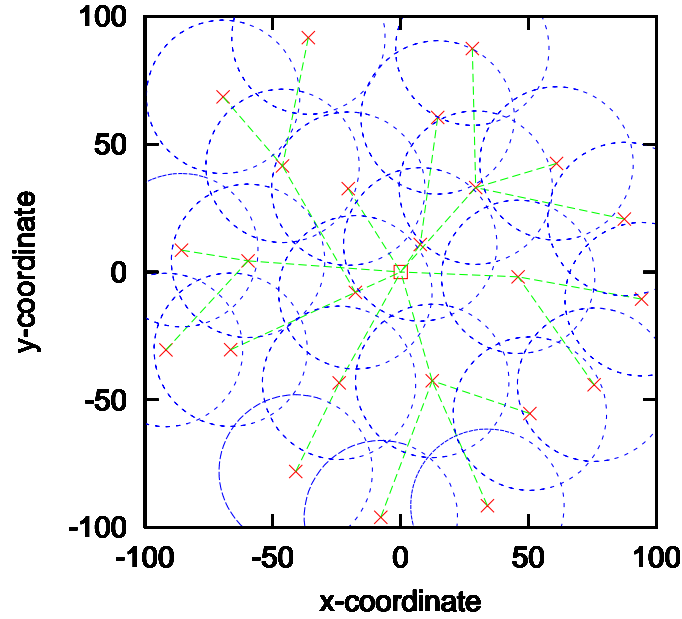


Figure 5: Overlapping clusters

Table 2: Parameters used in analysis

r	cluster radius (m)
k	size of sensor data (bit)
ρ	density of sensor nodes (nodes/m ²)
S	region that a cluster-head is responsible for in multihop transmission (m ²)
W	radius of sensor network (m)
t	distance between cluster-head and base station (m)

are edges of clusters. By assuming that half of the sensor nodes in an intersection region belong to one cluster and the other half to the other, we consider that the region from which a cluster-head gathers sensor data, which we call a cover region, becomes a square as illustrated in Fig. 6. When a diameter of cluster is r , the area becomes the square of r . In multihop communication, we assume that the distance from a cluster-head to the next-hop cluster-head is r .

All cluster members send their sensor data from k bits to their cluster-heads, even if the base station is closer to a member. In addition to the sensor data from its members and its own, a cluster-head has to receive and forward data of sensor nodes in its outer region S , which is illustrated in Fig. 7. The area of S is defined in accordance with the distance t of a cluster-head to a base station. When the radius is smaller than the twice the distance to the base station, $r < 2t$, the area of S

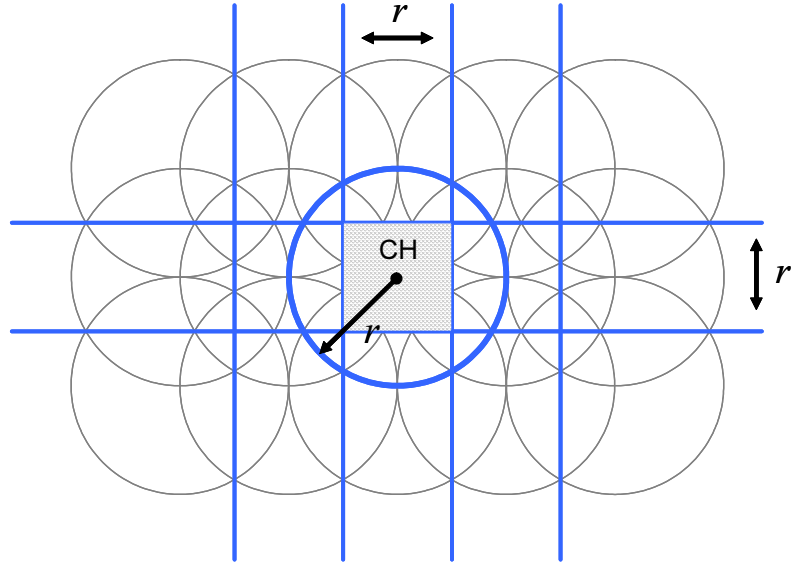
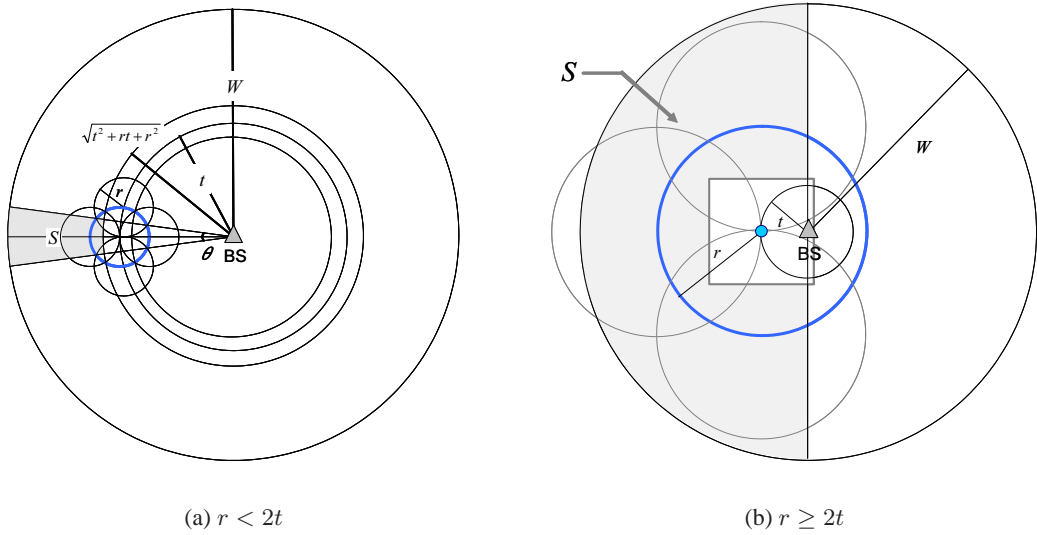


Figure 6: Region covered by one cluster



(a) $r < 2t$

(b) $r \geq 2t$

Figure 7: Region S that a cluster-head is responsible for

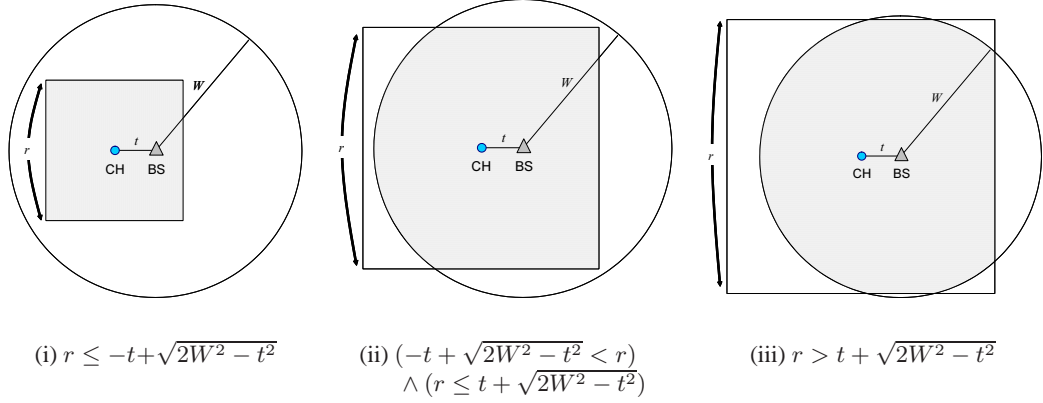


Figure 8: Three conditions among the cover region and the monitoring region

becomes a polar rectangle, formed by the sector of the annulus between two circles. It is enclosed by radius of the monitoring region and the left boundary of the cover region $\sqrt{t^2 + rt + r^2}$. The sides of the polar rectangle are given by the boundaries of the cover region to its upper and lower neighbors. On the other hand, when a cluster-head has a radius of $r \geq 2t$, we consider that it is responsible for the half of the monitoring region in multihop data gathering. Note that in this model, we do not consider either of data fusing or compression.

5.2 Derivation of $E_{all,m \rightarrow h}$

Depending on the relationship of r and W , there are three conditions between the cover region and the monitoring region as shown in Fig. 8. Among them, we consider only (i) and (ii), because it is unrealistic that the cluster radius r is much larger than the radius of the monitoring region W . When we consider the effect of multipath fading in Eq. (16), two conditions are further categorized into ten cases as shown in Figs. 9 and 10.

When $r \leq -t + \sqrt{2W^2 - t^2}$ holds, the whole cover region of a cluster fits within the monitoring region as illustrated in Fig. 8 (i). This condition is divided into the following three cases depending on the influence of multipath fading.

- (a) $r < \sqrt{2}d_0$
- (b) $\sqrt{2}d_0 \leq r \leq 2d_0$
- (c) $2d_0 < r$

On the other hand, when $r > -t + \sqrt{2W^2 - t^2}$ holds, a part of the cover region protrudes from the monitoring region as illustrated in Fig. 8 (ii). This condition is divided into the following seven cases.

- (d) $r < \sqrt{2}d_0$
- (e) $(\sqrt{2}d_0 \leq r \leq 2d_0) \wedge \left(\left(\frac{d_0^2 - W^2 - t^2}{2t} \leq -t - \frac{r}{2} \right) \vee (-W < -t - d_0) \right)$
- (f) $(\sqrt{2}d_0 \leq r \leq 2d_0) \wedge (-W \geq -t - d_0) \wedge \left(-t - \frac{r}{2} < \frac{d_0^2 - W^2 - t^2}{2t} < -t - \sqrt{d_0^2 - \frac{r^2}{4}} \right)$
- (g) $(\sqrt{2}d_0 \leq r \leq 2d_0) \wedge (-W \geq -t - d_0) \wedge \left(-t - \sqrt{d_0^2 - \frac{r^2}{4}} \leq \frac{d_0^2 - W^2 - t^2}{2t} - t + \sqrt{d_0^2 - \frac{r^2}{4}} \right)$
- (h) $(\sqrt{2}d_0 \leq r \leq 2d_0) \wedge (-W \geq -t - d_0) \wedge \left(-t + \sqrt{d_0^2 - \frac{r^2}{4}} \leq \frac{d_0^2 - W^2 - t^2}{2t} \right)$
- (i) $(2d_0 < r) \wedge (-t - d_0 \geq -W)$
- (j) $(2d_0 < r) \wedge (-t - d_0 < -W)$

In the following, for each of cases, we first derive the average amount of energy consumed in sending sensor data from a sensor node in a cover region to a cluster-head, $E_{m \rightarrow h}$. Then, the total of $E_{m \rightarrow h}$, i.e., $E_{all.m \rightarrow h}$ is derived.

In cases (a) through (c), the area $S_{cluster}$ from which a cluster-head gathers sensor data is given as:

$$S_{cluster} = r^2. \quad (21)$$

Case (a)

In this case, all cluster members consume energy in proportional to the square of the transmission distance.

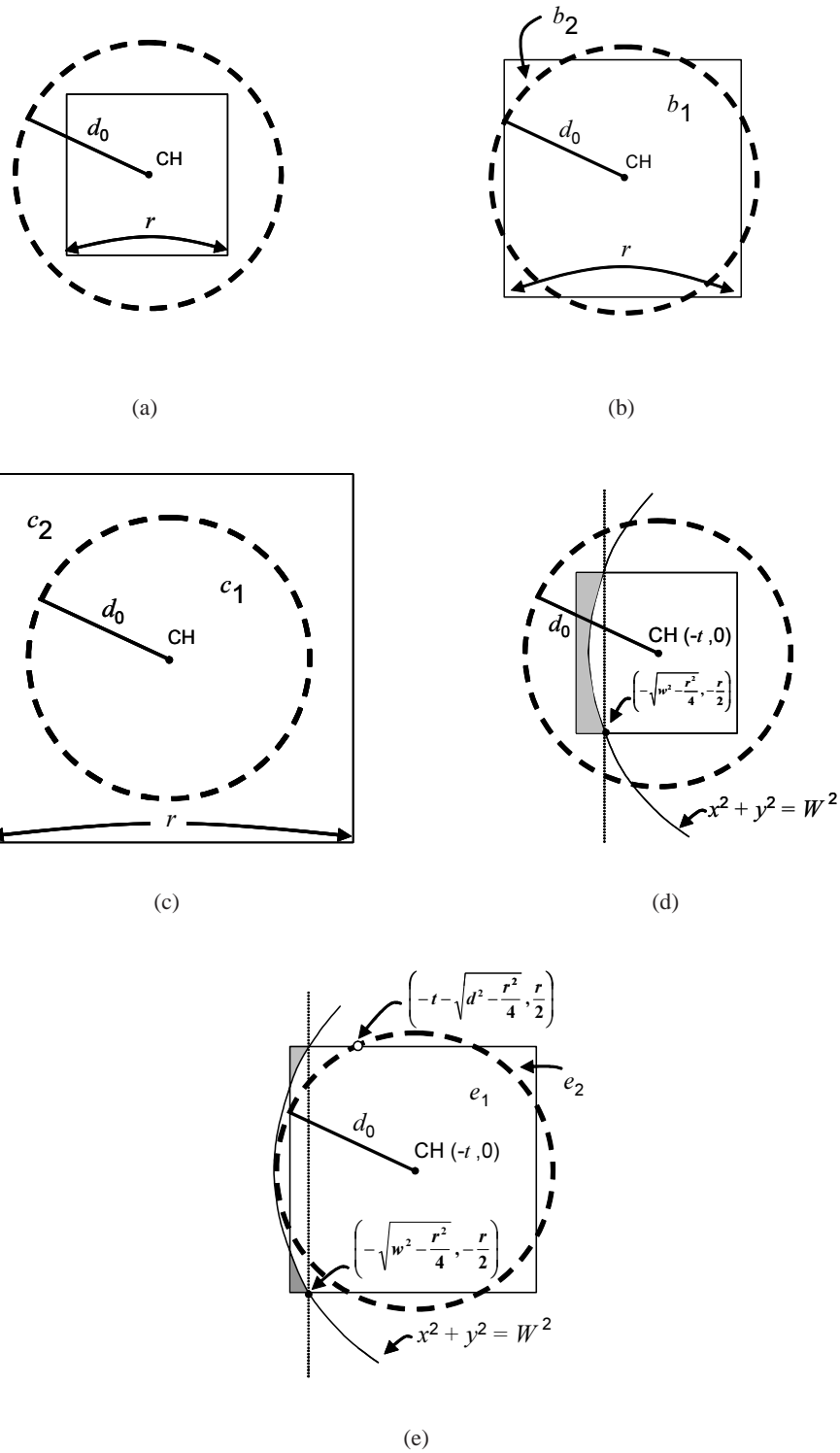
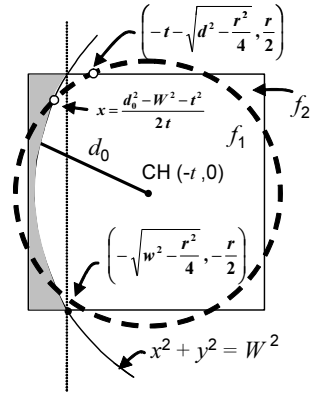
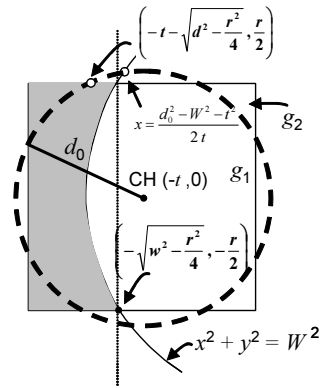


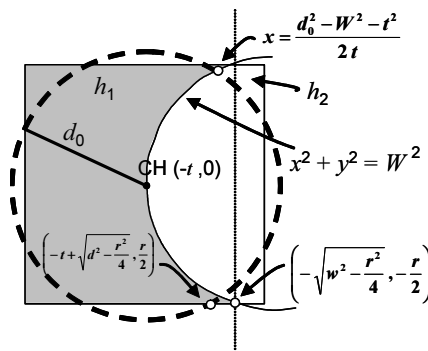
Figure 9: Cases of intra-cluster transmissions



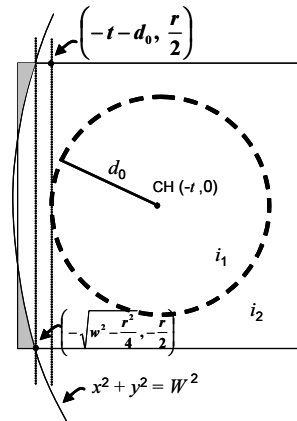
(f)



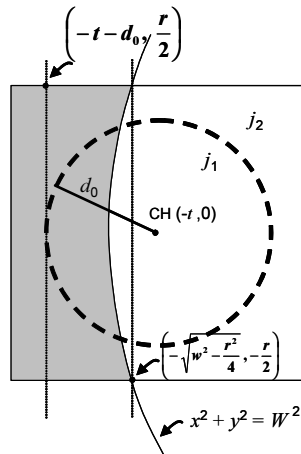
(g)



(h)



(i)



(j)

Figure 10: Cases of intra-cluster transmissions

$$\begin{aligned}
E_{m \rightarrow h} &= k \left\{ E_{elec} + \varepsilon_{fs} \int_{-\frac{r}{2}}^{\frac{r}{2}} \int_{-\frac{r}{2}}^{\frac{r}{2}} \frac{1}{S_{cluster}} (\sqrt{x^2 + y^2})^2 dx dy \right\} \\
&= k \left(E_{elec} + \frac{\varepsilon_{fs}}{S_{cluster}} \cdot \frac{r^4}{6} \right) \tag{22}
\end{aligned}$$

$$\begin{aligned}
E_{all_m \rightarrow h} &= (\rho S_{cluster} - 1) E_{m \rightarrow h} \approx \rho S_{cluster} E_{m \rightarrow h} \\
&= k \rho S_{cluster} \left(E_{elec} + \frac{\varepsilon_{fs}}{S_{cluster}} \cdot \frac{r^4}{6} \right) \\
&= k \rho \left(S_{cluster} \cdot E_{elec} + \varepsilon_{fs} \cdot \frac{r^4}{6} \right) \tag{23}
\end{aligned}$$

Case (b)

In this case, some of cluster members suffer from multipath fading. Let b_1 and b_2 correspond to the region where Eq. (15) and (16) apply, respectively. Their areas are denoted as S_{b_1} and S_{b_2} , respectively. The sum d_{b_1} of the square of the distance to the cluster-head of all sensor nodes in region b_1 is derived as:

$$\begin{aligned}
d_{b_1} &= 2 \int_{-\frac{r}{2}}^{-\sqrt{d_0^2 - \frac{r^2}{4}}} \int_{-\sqrt{d_0^2 - x^2}}^{\sqrt{d_0^2 - x^2}} (\sqrt{x^2 + y^2})^2 dy dx + \int_{-\sqrt{d_0^2 - \frac{r^2}{4}}}^{\frac{r}{2}} \int_{-\frac{r}{2}}^{\sqrt{d_0^2 - x^2}} (\sqrt{x^2 + y^2})^2 dy dx \\
&= -\frac{1}{12} \left[12d_0^4 \left\{ \arcsin\left(\frac{\sqrt{4d_0^2 - r^2}}{2d_0}\right) - \arcsin\left(\frac{r}{2d_0}\right) \right\} - r(r^2 + 2d_0^2)\sqrt{4d_0^2 - r^2} \right]. \tag{24}
\end{aligned}$$

The sum d_{b_2} of the fourth-power of the distance to the cluster-head of all sensor nodes in region b_2 is derived as:

$$\begin{aligned}
d_{b_2} &= 4 \int_{-\frac{r}{2}}^{-\sqrt{d_0^2 - \frac{r^2}{4}}} \int_{\sqrt{d_0^2 - x^2}}^{\frac{r}{2}} (\sqrt{x^2 + y^2})^4 dy dx \\
&= \frac{1}{180} \left[120d_0^6 \left\{ \arcsin\left(\frac{\sqrt{4d_0^2 - r^2}}{2d_0}\right) - \arcsin\left(\frac{r}{2d_0}\right) \right\} \right. \\
&\quad \left. - 2r(r^4 + 2d_0^2 r^2 + 6d_0^4)\sqrt{4d_0^2 - r^2} + 7r^6 \right]. \tag{25}
\end{aligned}$$

Then, $E_{m \rightarrow h}$ and $E_{all_m \rightarrow h}$ can be derived by the following equations.

$$\begin{aligned}
E_{m \rightarrow h} &= k \left(E_{elec} + \varepsilon_{fs} \cdot \frac{S_{b1}}{S_{cluster}} \cdot \frac{d_{b1}}{S_{b1}} + \varepsilon_{mp} \cdot \frac{S_{b2}}{S_{cluster}} \cdot \frac{d_{b2}}{S_{b2}} \right) \\
&= k \left(E_{elec} + \varepsilon_{fs} \cdot \frac{d_{b1}}{S_{cluster}} + \varepsilon_{mp} \cdot \frac{d_{b2}}{S_{cluster}} \right) \tag{26}
\end{aligned}$$

$$\begin{aligned}
E_{all_m \rightarrow h} &= (\rho S_{cluster} - 1) E_{m \rightarrow h} \approx \rho S_{cluster} E_{m \rightarrow h} \\
&= k \rho (S_{cluster} E_{elec} + \varepsilon_{fs} \cdot d_{b1} + \varepsilon_{mp} \cdot d_{b2}) \tag{27}
\end{aligned}$$

Case (c)

In this case, the whole region where the energy consumption is given by Eq. (15) is in a cover region of a cluster-head. Let c_1 and c_2 correspond to the region where Eq. (15) and Eq. (16) apply, respectively. Their areas are denoted as S_{c1} and S_{c2} , respectively. The sum d_{c1} of the square of the distance to the cluster-head of all sensor nodes in region c_1 is derived as:

$$d_{c1} = \int_0^{2\pi} \int_0^{d_0} r^3 dr d\theta = \frac{\pi d_0^4}{2}. \tag{28}$$

The sum d_{c2} of the fourth-power distance to the cluster-head of all sensor nodes in region c_2 is derived as:

$$\begin{aligned}
d_{c2} &= \int_{-\frac{r}{2}}^{\frac{r}{2}} \int_{-\frac{r}{2}}^{\frac{r}{2}} (\sqrt{x^2 + y^2})^4 dy dx - \int_0^{2\pi} \int_0^{d_0} r^5 dr d\theta \\
&= \frac{7r^6 - 60\pi d_0^6}{180}. \tag{29}
\end{aligned}$$

Then, $E_{m \rightarrow h}$ and $E_{all_m \rightarrow h}$ can be derived by the following equations.

$$\begin{aligned}
E_{m \rightarrow h} &= k \left\{ E_{elec} + \varepsilon_{fs} \cdot \left(\frac{S_{c1}}{S_{cluster}} \cdot \frac{d_{c1}}{S_{c1}} \right) + \varepsilon_{mp} \cdot \left(\frac{S_{c2}}{S_{cluster}} \cdot \frac{d_{c2}}{S_{c2}} \right) \right\} \\
&= k \left(E_{elec} + \frac{\varepsilon_{fs}}{S_{cluster}} \cdot d_{c1} + \frac{\varepsilon_{mp}}{S_{cluster}} \cdot d_{c2} \right) \tag{30}
\end{aligned}$$

$$\begin{aligned}
E_{all_m \rightarrow h} &= (\rho S_{cluster} - 1) \cdot E_{m \rightarrow h} \approx \rho S_{cluster} E_{m \rightarrow h} \\
&= k \rho (S_{cluster} \cdot E_{elec} + \varepsilon_{fs} \cdot d_{c1} + \varepsilon_{mp} \cdot d_{c2}) \tag{31}
\end{aligned}$$

In the following cases (d) through (j) where $r > -t + \sqrt{2W^2 - t^2}$ holds, a part of a cover region protrudes from the monitoring region. The area $S_{cluster}$ from which a cluster-head gathers

sensor data is derived as:

$$\begin{aligned}
S_{cluster} &= \frac{r}{2} \left(\sqrt{4W^2 - r^2} - 2t + r \right) + 2 \int_Z^{-\sqrt{W^2 - \frac{r^2}{4}}} \sqrt{W^2 - x^2} dx \\
&= -\frac{1}{4} \left[4W^2 \left\{ \arcsin\left(\frac{Z}{W}\right) + \arcsin\left(\frac{\sqrt{4W^2 - r^2}}{2W}\right) \right\} \right. \\
&\quad \left. + 4Z\sqrt{W^2 - Z^2} - r\sqrt{4W^2 - r^2} + 2r(2t - r) \right], \tag{32}
\end{aligned}$$

where Z is derived as:

$$Z = \max(-W, -t - \frac{r}{2}). \tag{33}$$

Case (d)

In this case, cluster members consume energy in proportion to the square of the transmission distance. Let d_1 correspond to the region covered by a cluster. The area is denoted as S_{d_1} ($= S_{cluster}$). The sum d_{d_1} of the square of the distance to the cluster-head of all sensor nodes in region d_1 is derived as:

$$\begin{aligned}
d_{d_1} &= \int_Z^{-\sqrt{W^2 - \frac{r^2}{4}}} \int_{-\sqrt{W^2 - x^2}}^{\sqrt{W^2 - x^2}} \left(\sqrt{(x+t)^2 + y^2} \right)^2 dy dx \\
&\quad + \int_{-\sqrt{W^2 - \frac{r^2}{4}}}^{-t + \frac{r}{2}} \int_{-\frac{r}{2}}^{\frac{r}{2}} \left(\sqrt{(x+t)^2 + y^2} \right)^2 dy dx \\
&= -\frac{1}{48} \left[24W^2(W^2 + 2t^2) \left\{ \arcsin\left(\frac{Z}{W}\right) + \arcsin\left(\frac{\sqrt{4W^2 - r^2}}{2W}\right) \right\} \right. \\
&\quad + 8(2Z^3 + 8tZ^2 + W^2Z + 6t^2Z - 8tW^2)\sqrt{W^2 - Z^2} \\
&\quad \left. - r(2W^2 + 12t^2 + r^2)\sqrt{4W^2 - r^2} + 4r(12tW^2 + 4t^3 - r^3) \right]. \tag{34}
\end{aligned}$$

$E_{m \rightarrow h}$ and $E_{all_m \rightarrow h}$ can be derived by the following equations.

$$\begin{aligned} E_{m \rightarrow h} &= k \left\{ E_{elec} + \varepsilon_{fs} \cdot \left(\frac{S_{d1}}{S_{cluster}} \cdot \frac{d_{d1}}{S_{d1}} \right) \right\} \\ &= k \left(E_{elec} + \frac{\varepsilon_{fs}}{S_{cluster}} \cdot d_{d1} \right) \end{aligned} \quad (35)$$

$$\begin{aligned} E_{all_m \rightarrow h} &= (\rho S_{cluster} - 1) \cdot E_{m \rightarrow h} \approx \rho S_{cluster} E_{m \rightarrow h} \\ &= k\rho (S_{cluster} \cdot E_{elec} + \varepsilon_{fs} \cdot d_{d1}) \end{aligned} \quad (36)$$

Case (e)

In this case, some of cluster members suffer from multipath fading. Let e_1 and e_2 correspond to the region where Eqs. (15) and (16) apply, respectively. Their areas are denoted as S_{e_1} and S_{e_2} , respectively. The sum d_{e_1} of the square of the distance to the cluster-head of all sensor nodes in region e_1 is derived as:

$$\begin{aligned} d_{e_1} &= d_{b_1} \\ &= -\frac{1}{12} \left[12d_0^4 \left\{ \arcsin\left(\frac{\sqrt{4d_0^2 - r^2}}{2d_0}\right) - \arcsin\left(\frac{r}{2d_0}\right) \right\} - r(r^2 + 2d_0^2)\sqrt{4d_0^2 - r^2} \right] \end{aligned} \quad (37)$$

The sum d_{e_2} of the fourth-power of the distance to the cluster-head of all sensor nodes in region e_2 is derived as:

$$\begin{aligned} d_{e_2} &= d_{b_2} - 2 \int_{-t-\frac{r}{2}}^{-\sqrt{W^2 - \frac{r^2}{4}}} \int_{\sqrt{W^2 - x^2}}^{\frac{r}{2}} \left(\sqrt{(x+t)^2 + y^2} \right)^4 dy dx \\ &= -\frac{1}{360} \left[120W^2(W^4 + 6t^2W^2 + 3t^4) \left\{ \arcsin\left(\frac{\sqrt{4W^2 - r^2}}{2W}\right) - \arcsin\left(\frac{2t+r}{2W}\right) \right\} \right. \\ &\quad + 240d_0^6 \left\{ \arcsin\left(\frac{r}{2d_0}\right) - \arcsin\left(\frac{\sqrt{4d_0^2 - r^2}}{2d_0}\right) \right\} \\ &\quad - \left\{ 2W^2(150tW^2 + 3rW^2 + 140t^3 - 66rt^2 - 6r^2t + r^3) \right. \\ &\quad \quad \left. + 20t^5 + 26rt^4 + 32r^2t^3 + 4r^3t^2 - 2r^4t + r^5 \right\} \sqrt{4W^2 - (2t+r)^2} \\ &\quad - r(6W^4 + 180t^2W^2 + 2r^2W^2 + 90t^4 + r^4)\sqrt{4W^2 - r^2} \\ &\quad + 4r(r^4 + 2d_0^2r^2 + 6d_0^4)\sqrt{4d_0^2 - r^2} \\ &\quad \left. + 360rtW^4 + 720rt^3W^2 + 72rt^5 - 40r^3t^3 - 7r^6 \right]. \end{aligned} \quad (38)$$

Then, $E_{m \rightarrow h}$ and $E_{all_m \rightarrow h}$ can be derived by the following equations.

$$\begin{aligned} E_{m \rightarrow h} &= k \left\{ E_{elec} + \varepsilon_{fs} \left(\frac{S_{e_1}}{S_{cluster}} \cdot \frac{d_{e_1}}{S_{e_1}} \right) + \varepsilon_{mp} \left(\frac{S_{e_2}}{S_{cluster}} \cdot \frac{d_{e_2}}{S_{e_2}} \right) \right\} \\ &= k \left(E_{elec} + \frac{\varepsilon_{fs}}{S_{cluster}} \cdot d_{e_1} + \frac{\varepsilon_{mp}}{S_{cluster}} \cdot d_{e_2} \right) \end{aligned} \quad (39)$$

$$\begin{aligned} E_{all_m \rightarrow h} &= (\rho S_{cluster} - 1) E_{m \rightarrow h} \approx \rho S_{cluster} E_{m \rightarrow h} \\ &= k \rho S_{cluster} \left(E_{elec} + \frac{\varepsilon_{fs}}{S_{cluster}} \cdot d_{e_1} + \frac{\varepsilon_{mp}}{S_{cluster}} \cdot d_{e_2} \right) \\ &= k \rho \left(S_{cluster} \cdot E_{elec} + \varepsilon_{fs} \cdot d_{e_1} + \varepsilon_{mp} \cdot d_{e_2} \right) \end{aligned} \quad (40)$$

Case (f)

In this case, some of the cluster members suffer from multipath fading. Let f_1 and f_2 correspond to the region where Eqs. (15) and (16) apply, respectively. Their areas are denoted as S_{f_1} and S_{f_2} , respectively. The sum d_{f_1} of the square of the distance to the cluster-head of all sensor nodes in region f_1 is derived as:

$$\begin{aligned} d_{f_1} &= d_{b_1} - \int_{Z_2}^{-W} \int_{-\sqrt{d_0^2 - (x+t)^2}}^{\sqrt{d_0^2 - (x+t)^2}} \left(\sqrt{(x+t)^2 + y^2} \right)^2 dy dx \\ &\quad - 2 \int_{Z_1}^{\frac{d_0^2 - W^2 - t^2}{2t}} \int_{\sqrt{W^2 - x^2}}^{\sqrt{d_0^2 - (x+t)^2}} \left(\sqrt{(x+t)^2 + y^2} \right)^2 dy dx \\ &= \frac{1}{24} \left[12d_0^4 \left\{ \arcsin\left(\frac{Z_2 + t}{d_0}\right) + \arcsin\left(\frac{Z_1 + t}{d_0}\right) + \arcsin\left(\frac{W^2 - t^2 - d_0^2}{2d_0 t}\right) \right. \right. \\ &\quad \left. \left. + \arcsin\left(\frac{W - t}{d_0}\right) + 2 \arcsin\left(\frac{r}{2d_0}\right) - 2 \arcsin\left(\frac{\sqrt{4d_0^2 - r^2}}{2d_0}\right) \right\} \right. \\ &\quad \left. - 12W^2(W^2 + 2t^2) \left\{ k \arcsin\left(\frac{Z_1}{W}\right) + \arcsin\left(\frac{W^2 + t^2 - d_0^2}{2tW}\right) \right\} \right. \\ &\quad + 4(2Z_2^3 + 6tZ_2^2 + 6t^2Z_2 + d_0^2Z_2 + 2t^3 + d_0^2t) \sqrt{d_0^2 - (Z_2 + t)^2} \\ &\quad + 4(2Z_1^3 + 6tZ_1^2 + 6t^2Z_1 + d_0^2Z_1 + 2t^3 + d_0^2t) \sqrt{d_0^2 - (Z_1 + t)^2} \\ &\quad - 3(5W^2 + t^2 + d_0^2) \sqrt{-W^4 + 2(d_0^2 + t^2)W^2 - (t^2 - d_0^2)^2} \\ &\quad + 4(2W^3 - 6tW^2 + 6t^2W + d_0^2W - 2t^3 - d_0^2t) \sqrt{d_0^2 - (W - t)^2} \\ &\quad \left. - 4(2Z_1^3 + 8Z_1^2t + W^2Z_1 + 6t^2Z_1 - 8tW^2) \sqrt{W^2 - Z_1^2} + r(2r^2 + 4d_0^2) \sqrt{4d_0^2 - r^2} \right]. \end{aligned} \quad (41)$$

The sum d_{f_2} of the fourth-power of the distance to the cluster-head of all sensor nodes in region f_2 is derived as:

$$\begin{aligned}
d_{f_2} &= d_{b_2} - 2 \int_{-t-\frac{r}{2}}^{\frac{d_0^2-W^2-t^2}{2t}} \int_{\sqrt{d_0^2-(x+t)^2}}^{\frac{r}{2}} \left(\sqrt{(x+t)^2+y^2} \right)^4 dy dx \\
&\quad - 2 \int_{\frac{d_0^2-W^2-t^2}{2t}}^{-\sqrt{W^2-\frac{r^2}{4}}} \int_{\sqrt{W^2-x^2}}^{\frac{r}{2}} \left(\sqrt{(x+t)^2+y^2} \right)^4 dy dx \\
&= \frac{-1}{360} \left[120W^2(W^4 + 6t^2W^2 + 3t^4) \left\{ \arcsin\left(\frac{\sqrt{4W^2-r^2}}{2W}\right) - \arcsin\left(\frac{W^2+t^2-d^2}{2tW}\right) \right\} \right. \\
&\quad \left. 120d_0^6 \left\{ \arcsin\left(\frac{W^2-t^2-d_0^2}{2d_0t}\right) - 2 \arcsin\left(\frac{\sqrt{4d_0^2-r^2}}{2d_0}\right) + \arcsin\left(\frac{r}{2d_0}\right) \right\} \right. \\
&\quad - 20(10W^4 + 19t^2W^2 + 4d_0^2W^2 + t^4 + d_0^2t^2 + d_0^4) \sqrt{-W^4 + 2(t^2 + d_0^2)W^2 - (t^2 - d_0^2)^2} \\
&\quad - r(6W^4 + 180t^2W^2 + 2r^2W^2 + 90t^4 + r^4) \sqrt{4W^2 - r^2} \\
&\quad \left. + 3r(r^4 + 2d_0^2r^2 + 6d_0^4) \sqrt{4d_0^2 - r^2} + r(360tW^4 + 720t^3W^2 + 72t^5 - 40r^2t^3 - 7r^5) \right], \tag{42}
\end{aligned}$$

where, Z_1 and Z_2 correspond to $Z_1 = \max(-W, -t - \frac{r}{2})$ and $Z_2 = \min(-W, -t - \frac{r}{2})$, respectively. Then, $E_{m \rightarrow h}$ and $E_{all_m \rightarrow h}$ can be derived by the following equations.

$$\begin{aligned}
E_{m \rightarrow h} &= k \left\{ E_{elec} + \varepsilon_{fs} \left(\frac{S_{f_1}}{S_{cluster}} \cdot \frac{d_{f_1}}{S_{f_1}} \right) + \varepsilon_{mp} \left(\frac{S_{f_2}}{S_{cluster}} \cdot \frac{d_{f_2}}{S_{f_2}} \right) \right\} \\
&= k \left(E_{elec} + \frac{\varepsilon_{fs}}{S_{cluster}} \cdot d_{f_1} + \frac{\varepsilon_{mp}}{S_{cluster}} \cdot d_{f_2} \right) \tag{43}
\end{aligned}$$

$$\begin{aligned}
E_{all_m \rightarrow h} &= (\rho S_{cluster} - 1) E_{m \rightarrow h} \approx \rho S_{cluster} E_{m \rightarrow h} \\
&= k \rho S_{cluster} \left(E_{elec} + \frac{\varepsilon_{fs}}{S_{cluster}} \cdot d_{f_1} + \frac{\varepsilon_{mp}}{S_{cluster}} \cdot d_{f_2} \right) \\
&= k \rho (S_{cluster} \cdot E_{elec} + \varepsilon_{fs} \cdot d_{f_1} + \varepsilon_{mp} \cdot d_{f_2}) \tag{44}
\end{aligned}$$

Case (g)

In this case, some of the cluster members suffer from multipath fading. Let g_1 and g_2 correspond to the region where Eqs. (15) and (16) apply, respectively. Their areas are denoted as S_{g_1} and S_{g_2} , respectively. The sum d_{g_1} of the square of the distance to the cluster-head of all sensor nodes in

region g_1 is derived as:

$$\begin{aligned}
d_{g_1} &= \int_Z^{-\sqrt{W^2 - \frac{r^2}{4}}} \int_{-\sqrt{W^2 - x^2}}^{\sqrt{W^2 - x^2}} \left(\sqrt{(x+t)^2 + y^2} \right)^2 dy dx \\
&+ \int_{-\sqrt{W^2 - \frac{r^2}{4}}}^{-t + \sqrt{\frac{d_0^2 - r^2}{4}}} \int_{-\frac{r}{2}}^{\frac{r}{2}} \left(\sqrt{(x+t)^2 + y^2} \right)^2 dy dx \\
&+ \int_{-t + \sqrt{\frac{d_0^2 - r^2}{4}}}^{-t + \frac{r}{2}} \int_{-\sqrt{d_0^2 - (x+t)^2}}^{\sqrt{d_0^2 - (x+t)^2}} \left(\sqrt{(x+t)^2 + y^2} \right)^2 dy dx \\
&= -\frac{1}{48} \left[24W^2(W^2 + 2t^2) \left\{ \arcsin\left(\frac{Z}{W}\right) + \arcsin\left(\frac{\sqrt{4W^2 - r^2}}{2W}\right) \right\} \right. \\
&\quad + 24d_0^4 \left\{ \arcsin\left(\frac{\sqrt{4d_0^2 - r^2}}{2d_0}\right) - \arcsin\left(\frac{r}{2d_0}\right) \right\} \\
&\quad + 8(2Z^3 + 8tZ^2 + W^2Z + 6t^2Z - 8tW^2)\sqrt{W^2 - Z^2} \\
&\quad \left. - r(2W^2 + 6t^2 + r^2)\sqrt{4W^2 - r^2} - 2r(r^2 + 2d_0^2)\sqrt{4d_0^2 - r^2} + 16rt(3W^2 + t^2) \right]. \tag{45}
\end{aligned}$$

The sum d_{g_2} of the fourth-power of the distance to the cluster-head of all sensor nodes in region g_2 is derived as:

$$\begin{aligned}
d_{g_2} &= \frac{1}{2} d_{b_2} \\
&= \frac{1}{360} \left[120d_0^6 \left\{ \arcsin\left(\frac{\sqrt{4d_0^2 - r^2}}{2d_0}\right) - \arcsin\left(\frac{r}{2d_0}\right) \right\} \right. \\
&\quad \left. - 2r(r^4 + 2d_0^2r^2 + 6d_0^4)\sqrt{4d_0^2 - r^2} + 7r^6 \right]. \tag{46}
\end{aligned}$$

Then, $E_{m \rightarrow h}$ and $E_{all_m \rightarrow h}$ can be derived by the following equations.

$$\begin{aligned}
E_{m \rightarrow h} &= k \left\{ E_{elec} + \varepsilon_{fs} \left(\frac{S_{g_1}}{S_{cluster}} \cdot \frac{d_{g_1}}{S_{g_1}} \right) + \varepsilon_{mp} \left(\frac{S_{g_2}}{S_{cluster}} \cdot \frac{d_{g_2}}{S_{g_2}} \right) \right\} \\
&= k \left(E_{elec} + \frac{\varepsilon_{fs}}{S_{cluster}} \cdot d_{g_1} + \frac{\varepsilon_{mp}}{S_{cluster}} \cdot d_{g_2} \right) \tag{47}
\end{aligned}$$

$$\begin{aligned}
E_{all_m \rightarrow h} &= (\rho S_{cluster} - 1) E_{m \rightarrow h} \approx \rho S_{cluster} E_{m \rightarrow h} \\
&= k \rho S_{cluster} \left(E_{elec} + \frac{\varepsilon_{fs}}{S_{cluster}} \cdot d_{g_1} + \frac{\varepsilon_{mp}}{S_{cluster}} \cdot d_{g_2} \right) \\
&= k \rho (S_{cluster} \cdot E_{elec} + \varepsilon_{fs} \cdot d_{g_1} + \varepsilon_{mp} \cdot d_{g_2}) \tag{48}
\end{aligned}$$

Case (h)

In this case, some of the cluster members suffer from multipath fading. Let h_1 and h_2 correspond to the region where Eqs. (15) and (16) apply, respectively. Their areas are denoted as S_{h_1} and S_{h_2} , respectively. The sum d_{h_1} of the square of the distance to the cluster-head of all sensor nodes in region h_1 is derived as:

$$\begin{aligned}
d_{h_1} &= \int_{-W}^{\frac{d_0^2 - W^2 - t^2}{2t}} \int_{-\sqrt{W^2 - x^2}}^{\sqrt{W^2 - x^2}} \left(\sqrt{(x+t)^2 + y^2} \right)^2 dy dx \\
&\quad + \int_{\frac{d_0^2 - W^2 - t^2}{2t}}^{-t+r/2} \int_{-\sqrt{d_0^2 - (x+t)^2}}^{\sqrt{d_0^2 - (x+t)^2}} \left(\sqrt{(x+t)^2 + y^2} \right)^2 dy dx \\
&= -\frac{1}{48} \left[24W^2(W^2 + 2t^2) \left\{ \arcsin\left(\frac{Z}{W}\right) - \frac{\pi}{2} \right\} \right. \\
&\quad \left. - 24d_0^4 \left\{ \arcsin\left(\frac{W^2 - t^2 - d_0^2}{2d_0 t}\right) + \arcsin\left(\frac{r}{2d_0}\right) \right\} \right. \\
&\quad \left. + 6(5W^2 + t^2 + d_0^2) \sqrt{-W^4 + 2(t^2 + d_0^2)W^2 - (t^2 - d_0^2)^2} - r(r^2 + 2d_0^2) \sqrt{4d_0^2 - r^2} \right]. \tag{49}
\end{aligned}$$

The sum d_{h_2} of the fourth-power of the distance to the cluster-head of all sensor nodes in region h_2 is derived as:

$$\begin{aligned}
d_{h_2} &= 2 \int_{\frac{d_0^2 - W^2 - t^2}{2t}}^{-\sqrt{W^2 - \frac{r^2}{4}}} \int_{\sqrt{d_0^2 - (x+t)^2}}^{\sqrt{W^2 - x^2}} \left(\sqrt{(x+t)^2 + y^2} \right)^4 dy dx \\
&\quad + 2 \int_{-\sqrt{W^2 - \frac{r^2}{4}}}^{-t+\frac{r}{2}} \int_{\sqrt{d_0^2 - (x+t)^2}}^{\frac{r}{2}} \left(\sqrt{(x+t)^2 + y^2} \right)^4 dy dx \\
&= -\frac{1}{360} \left[120W^2(W^4 + 6t^2W^2 + 3t^4) \left\{ \arcsin\left(\frac{\sqrt{4W^2 - r^2}}{2W}\right) - \arcsin\left(\frac{W^2 + t^2 - d_0^2}{2tW}\right) \right\} \right. \\
&\quad \left. 160d_0^6 \left\{ \arcsin\left(\frac{W^2 - t^2 - d_0^2}{2d_0 t}\right) - \arcsin\left(\frac{r}{2d_0}\right) \right\} \right. \\
&\quad - 20(20W^4 + 19t^2W^2 + 4d_0^2W^2 + 90t^4 + t^4 + d_0^2t^2 + d_0^4) \sqrt{-W^4 + 2(t^2 + d_0^2)W^2 - (t^2 - d_0^2)^2} \\
&\quad - r(6W^4 + 180t^2W^2 + 2r^2W^2 + 90t^4 + r^4) \sqrt{4W^2 - r^2} \\
&\quad + r(r^4 + 2d_0^2r^2 + 6d_0^4) \sqrt{4d_0^2 - r^2} \\
&\quad \left. + r(360tW^4 + 720t^3W^2 + 72t^5 - 40r^2t^3 - 7r^5) \right]. \tag{50}
\end{aligned}$$

Then, $E_{m \rightarrow h}$ and $E_{all_m \rightarrow h}$ can be derived by the following equations.

$$\begin{aligned}
E_{m \rightarrow h} &= k \left\{ E_{elec} + \varepsilon_{fs} \left(\frac{S_{h_1}}{S_{cluster}} \cdot \frac{d_{h_1}}{S_{h_1}} \right) + \varepsilon_{mp} \left(\frac{S_{h_2}}{S_{cluster}} \cdot \frac{d_{h_2}}{S_{h_2}} \right) \right\} \\
&= k \left(E_{elec} + \frac{\varepsilon_{fs}}{S_{cluster}} \cdot d_{h_1} + \frac{\varepsilon_{mp}}{S_{cluster}} \cdot d_{h_2} \right)
\end{aligned} \tag{51}$$

$$\begin{aligned}
E_{all_m \rightarrow h} &= (\rho S_{cluster} - 1) E_{m \rightarrow h} \approx \rho S_{cluster} E_{m \rightarrow h} \\
&= k \rho S_{cluster} \left(E_{elec} + \frac{\varepsilon_{fs}}{S_{cluster}} \cdot d_{h_1} + \frac{\varepsilon_{mp}}{S_{cluster}} \cdot d_{h_2} \right) \\
&= k \rho (S_{cluster} \cdot E_{elec} + \varepsilon_{fs} \cdot d_{h_1} + \varepsilon_{mp} \cdot d_{h_2})
\end{aligned} \tag{52}$$

Case (i)

In this case, some of cluster members suffer from multipath fading. Let i_1 and i_2 correspond to the region where Eqs. (15) and (16) apply, respectively. Their areas are denoted as S_{i_1} and S_{i_2} , respectively. The sum d_{i_1} of the square of the distance to the cluster-head of all sensor nodes in region h_1 is derived as:

$$d_{i_1} = d_{S_{c1}} = \frac{\pi d_0^4}{2}. \tag{53}$$

The sum d_{i_2} of the fourth-power of the distance to the cluster-head of all sensor nodes in region

i_2 is derived as:

$$\begin{aligned}
d_{i_2} &= d_{S_{c2}}^4 - \int_{Z_2}^{-W} \int_{-\frac{r}{2}}^{\frac{r}{2}} \left(\sqrt{(x+t)^2 + y^2} \right)^4 dy dx \\
&\quad - 2 \int_{Z_1}^{-\sqrt{W^2 - \frac{r^2}{4}}} \int_{\sqrt{W^2 - x^2}}^{\frac{r}{2}} \left(\sqrt{(x+t)^2 + y^2} \right)^4 dy dx \\
&= \frac{1}{720} \left[-240W^2(W^4 + 6t^2W^2 + 3t^4) \left\{ \arcsin\left(\frac{Z_1}{W}\right) + \arcsin\left(\frac{\sqrt{4W^2 - r^2}}{2W}\right) \right\} \right. \\
&\quad - 16 \left(8Z_1^5 + 48tZ_1^4 + 4W^2Z_1^3 + 120t^2Z_1^3 + 24tW^2Z_1^2 + 120t^3Z_1^2 \right. \\
&\quad \quad \left. \left. + 3W^4Z_1 - 30t^2W^2Z_1 + 45t^4Z_1 - 72tW^4 - 120t^3W^2 \right) \sqrt{W^2 - Z_1^2} \right. \\
&\quad + 2r \left(6W^4 + 180t^2W^2 + 2r^2W^2 + 90t^4 + r^4 \right) \sqrt{4W^2 - r^2} \\
&\quad + r \left(144Z_2^5 + 720tZ_2^4 + 1440t^2Z_2^3 + 40r^2Z_2^3 + 1440t^3Z_2^2 \right. \\
&\quad \quad \left. + 120r^2tZ_2^2 + 720t^4Z_2 + 120r^2t^2Z_2 + 9r^4Z_2 \right) \\
&\quad + r \left(144Z_1^5 + 720tZ_1^4 + 1440t^2Z_1^3 + 40r^2Z_1^3 + 1440t^3Z_1^2 \right. \\
&\quad \quad \left. + 120r^2tZ_1^2 + 720t^4Z_1 + 120r^2t^2Z_1 + 9r^4Z_1 \right) \\
&\quad + 144rW^5 - 1440rtW^4 + 1440rt^2W^3 + 40r^3W^3 - 2880rt^3W^2 - 120r^3tW^2 \\
&\quad \left. + 720rt^4W + 120r^3t^2W + 9r^5W + 120r^3t^3 + 9r^5t + 28r^6 - 240d_0^6\pi \right], \tag{54}
\end{aligned}$$

where, $Z_1 = \max(-W, -t - \frac{r}{2})$ and $Z_2 = \min(-W, -t - \frac{r}{2})$.

Then, $E_{m \rightarrow h}$ and $E_{all_m \rightarrow h}$ can be derived by the following equations.

$$\begin{aligned}
E_{m \rightarrow h} &= k \left\{ E_{elec} + \varepsilon_{fs} \left(\frac{S_{i_1}}{S_{cluster}} \cdot \frac{d_{i_1}}{S_{i_1}} \right) + \varepsilon_{mp} \left(\frac{S_{i_2}}{S_{cluster}} \cdot \frac{d_{i_2}}{S_{i_2}} \right) \right\} \\
&= k \left(E_{elec} + \frac{\varepsilon_{fs}}{S_{cluster}} \cdot d_{i_1} + \frac{\varepsilon_{mp}}{S_{cluster}} \cdot d_{i_2} \right) \tag{55}
\end{aligned}$$

$$\begin{aligned}
E_{all_m \rightarrow h} &= (\rho S_{cluster} - 1) E_{m \rightarrow h} \approx \rho S_{cluster} E_{m \rightarrow h} \\
&= k \rho S_{cluster} \left(E_{elec} + \frac{\varepsilon_{fs}}{S_{cluster}} \cdot d_{i_1} + \frac{\varepsilon_{mp}}{S_{cluster}} \cdot d_{i_2} \right) \\
&= k \rho (S_{cluster} \cdot E_{elec} + \varepsilon_{fs} \cdot d_{i_1} + \varepsilon_{mp} \cdot d_{i_2}) \tag{56}
\end{aligned}$$

Case (j)

In this case, some of the cluster members suffer from multipath fading. Let j_1 and j_2 correspond

to the region where Eqs. (15) and (16) apply, respectively. Their areas are denoted as S_{j_1} and S_{j_2} , respectively. The sum d_{j_1} of the square of the distance to the cluster-head of all sensor nodes in region j_1 is derived as:

$$\begin{aligned}
d_{j_1} &= \int_{-W}^{\frac{d_0^2 - W^2 - t^2}{2t}} \int_{-\sqrt{W^2 - x^2}}^{\sqrt{W^2 - x^2}} \left(\sqrt{(x+t)^2 + y^2} \right)^2 dy dx \\
&\quad + \int_{\frac{d_0^2 - W^2 - t^2}{2t}}^{-t+d_0} \int_{-\sqrt{d_0^2 - (x+t)^2}}^{\sqrt{d_0^2 - (x+t)^2}} \left(\sqrt{(x+t)^2 + y^2} \right)^2 dy dx \\
&= -\frac{1}{8} \left[4W^2(W^2 + 2t^2) \left\{ \arcsin\left(\frac{W^2 + t^2 - d_0^2}{2tW}\right) - \frac{\pi}{2} \right\} - 2\pi d_0^4 \right. \\
&\quad \left. - 4d_0^4 \arcsin\left(\frac{W^2 - t^2 - d_0^2}{2d_0 t}\right) + (5W^2 + t^2 + d_0^2) \sqrt{-W^4 + 2(t^2 + d_0^2)W^2 - (t^2 - d_0^2)^2} \right]. \tag{57}
\end{aligned}$$

The sum d_{j_2} of the fourth-power of the distance to the cluster-head of all sensor nodes in region j_2 is derived as:

$$\begin{aligned}
d_{j_2} &= d_{c_2} - \int_{-t-\frac{r}{2}}^{-t-d_0} \int_{-\frac{r}{2}}^{\frac{r}{2}} \left(\sqrt{(x+t)^2 + y^2} \right)^4 dy dx \\
&\quad - 2 \int_{-t-d_0}^{\frac{d_0^2 - W^2 - t^2}{2t}} \int_{-\sqrt{d_0^2 - (x+t)^2}}^{\frac{r}{2}} \left(\sqrt{(x+t)^2 + y^2} \right)^4 dy dx \\
&\quad - 2 \int_{\frac{d_0^2 - W^2 - t^2}{2t}}^{-\sqrt{W^2 - \frac{r^2}{4}}} \int_{\sqrt{W^2 - x^2}}^{\frac{r}{2}} \left(\sqrt{(x+t)^2 + y^2} \right)^4 dy dx \\
&= -\frac{1}{360} \left[120W^2(W^4 + 6t^2W^2 + 3t^4) \left\{ \arcsin\left(\frac{\sqrt{4W^2 - r^2}}{2W}\right) - \arcsin\left(\frac{W^2 + t^2 - d_0^2}{2tW}\right) \right\} \right. \\
&\quad + 120d_0^6 \arcsin\left(\frac{W^2 - t^2 - d_0^2}{2d_0 t}\right) \\
&\quad - 20(10W^4 + 19t^2W^2 + 4d_0^2W^2 + t^4 + d_0^2t^2 + d_0^4) \sqrt{-W^4 + 2(t^2 + d_0^2)W^2 - (t^2 - d_0^2)^2} \\
&\quad - r(6W^4 + 180t^2W^2 + 2r^2W^2 + 90t^4 + r^4) \sqrt{4W^2 - r^2} \\
&\quad \left. + 360rtW^4 + 720rt^3W^2 + 72rt^5 - 40r^3t^3 - 7r^6 + 60d_0^6\pi \right]. \tag{58}
\end{aligned}$$

Then, $E_{m \rightarrow h}$ and $E_{all_m \rightarrow h}$ can be derived by the following equations.

$$\begin{aligned} E_{m \rightarrow h} &= k \left\{ E_{elec} + \varepsilon_{fs} \left(\frac{S_{j_1}}{S_{cluster}} \cdot \frac{d_{j_1}}{S_{j_1}} \right) + \varepsilon_{mp} \left(\frac{S_{g_2}}{S_{cluster}} \cdot \frac{d_{j_2}}{S_{j_2}} \right) \right\} \\ &= k \left(E_{elec} + \frac{\varepsilon_{fs}}{S_{cluster}} \cdot d_{S_{j_1}}^2 + \frac{\varepsilon_{mp}}{S_{cluster}} \cdot d_{S_{j_2}}^4 \right) \end{aligned} \quad (59)$$

$$\begin{aligned} E_{all_m \rightarrow h} &= (\rho S_{cluster} - 1) E_{m \rightarrow h} \approx \rho S_{cluster} E_{m \rightarrow h} \\ &= k \rho S_{cluster} \left(E_{elec} + \frac{\varepsilon_{fs}}{S_{cluster}} \cdot d_{j_1} + \frac{\varepsilon_{mp}}{S_{cluster}} \cdot d_{j_2} \right) \\ &= k \rho (S_{cluster} \cdot E_{elec} + \varepsilon_{fs} \cdot d_{j_1} + \varepsilon_{mp} \cdot d_{j_2}) \end{aligned} \quad (60)$$

5.3 Derivation of E_{head1}

The amount of energy E_{head1} consumed by a cluster-head in receiving sensor data from its members is derived as:

$$E_{head1} = k(\rho S_{cluster} - 1) E_{elec} \approx k \rho S_{cluster} E_{elec} \quad (61)$$

5.4 Derivation of E_{head2}

E_{head2} corresponds to the energy consumed by a cluster-head in receiving sensor data from outside cluster-heads. The area S where sensor data to forward exists is calculated as following. When the relationship between the cluster radius r and the distance of the cluster-head to a base station t satisfies $r < 2t$, S takes the form illustrated in Fig. 7 (a). When $r \geq 2t$ holds, S becomes the half of the monitoring region as illustrated in Fig. 7 (b). In case that $r \geq \frac{-t + \sqrt{4W^2 - 3t^2}}{2}$ holds, S becomes 0. Therefore, S can be derived as:

$$S = \begin{cases} \frac{\theta}{2} (W^2 - t^2 - rt - r^2), & \text{if } (r < 2t) \wedge (r < \frac{-t + \sqrt{4W^2 - 3t^2}}{2}) \\ 0, & \text{if } (r < 2t) \wedge (r \geq \frac{-t + \sqrt{4W^2 - 3t^2}}{2}) \\ \frac{1}{2} \{ \pi W^2 + r^2 - 2(S_{cluster} + rt) \}, & \text{otherwise} \end{cases} \quad (62)$$

where θ is derived as:

$$\theta = \arccos \left(1 - \frac{r^2}{2t^2} \right). \quad (63)$$

The total amount K of sensor data that a cluster-head receives from region S is given as:

$$K = k\rho S.$$

Therefore, the energy E_{head2} consumed in reception of sensor data from other cluster-heads is given as:

$$\begin{aligned} E_{head2} &= KE_{elec} \\ &= k\rho SE_{elec}. \end{aligned} \quad (64)$$

5.5 Derivation of E_{head3}

A cluster-head sends all sensor data to the next-hop, a cluster-head or the base station. The distance to the next-hop is r , if $r > t$ holds, or t , i.e., direct transmission.

If either of $r < d_0$ or $r \geq d_0 > t$ holds, a cluster-head consumes energy which scales proportionally to the square of the transmission distance. Therefore, E_{head3} consumed in transmission of sensor data is derived as:

$$\begin{aligned} E_{head3} &= (k\rho S_{cluster} + K) \{E_{elec} + \varepsilon_{fs} \cdot \min(r^2, t^2)\} \\ &= k\rho(S_{cluster} + S) \{E_{elec} + \varepsilon_{fs} \cdot \min(r^2, t^2)\}. \end{aligned} \quad (65)$$

Otherwise, a cluster-head consumes energy which scales proportionally to the fourth power of the transmission distance.

$$\begin{aligned} E_{head3} &= (k\rho S_{cluster} + K) \{E_{elec} + \varepsilon_{mp} \cdot \min(r^4, t^4)\} \\ &= k\rho(S_{cluster} + S) \{E_{elec} + \varepsilon_{mp} \cdot \min(r^4, t^4)\}. \end{aligned} \quad (66)$$

5.6 Results of the Analysis

In Figs. 11 through 16, we show $E_{cluster}$ and E_{node} with radius r against the different size of the monitoring region W and the distance t of the cluster-head to the base station. The radius W was set at 100, 200, and 400. The distance t was set at 10%, 20%, 40%, and 80% of W . We set E_{elec} at 50 (nJ/bit), ε_{fs} at 10 (pJ/bit/m²), and ε_{mp} at 0.0013 (pJ/bit/m⁴) in Eqs. (15) through (17). The

threshold d_0 was set at 75 (m) [3].

First, from Figs. 11, 13 and 15, we observe that the amount of energy consumed in a cluster $E_{cluster}$ increases as radius r increases when $r < t$ holds, that is, the radius is smaller than the distance to the base station. This is because all of $E_{all_m \rightarrow h}$, E_{head1} , E_{head2} , and E_{head3} increase as radius r increases. When $r \geq t$ holds, that is, the base station exists in a cluster, a cluster-head sends the aggregated sensor data directly to the base station. Therefore, the slope becomes gentle against the increase of radius r . When radius r is equal to $2t$, the region for which a cluster-head is responsible in multihop communications changes from Fig. 7 (a) to Fig. 7 (b). Thus, in our model, $E_{cluster}$ suddenly increases. When radius r goes beyond $2t$ ($r > 2t$), $E_{all_m \rightarrow h}$ and E_{head1} keep increasing whereas E_{head2} and the distance to the next hop, i.e., the base station, do not change. Consequently, $E_{cluster}$ slowly increases.

Next, we consider the effect of the relationship among radius r and threshold d_0 on the energy consumption per node, E_{node} . When $r < d_0$ holds, the amount of energy that cluster members consume in transmitting their sensor data to a cluster-head is derived by Eq. (15). As radius r increases, the number of cluster members also increases. The total energy consumed in a cluster, $E_{cluster}$, also increases, but its rate of increase is slower than that of the number of cluster members. Therefore, E_{node} decreases with the increase of radius r as far as the whole cover region is within the monitoring region. On the other hand, when radius r is larger than threshold d_0 ($r \geq d_0$), the energy consumption in data transmission of some cluster members scales proportionally to the fourth-power of the distance. Thus, Eq. (16) applies. As a result, E_{node} increases as radius r increases. The reason why we observe sudden drops of E_{node} at threshold d_0 is that the energy derived by Eq. (15) is larger than the energy derived by Eq. (16) at threshold d_0 .

Finally, we consider the effect of the relation between radius r and distance t on the energy consumption per node, E_{node} . When the base station is within the range of radio signals, i.e., $r \geq t$, a cluster-head directly sends the aggregated data to the base station. Therefore, the increase rate of $E_{cluster}$ becomes small whereas the number of sensor nodes in a cluster keeps increasing at the rate of the square of the radius. Consequently, E_{node} decreases as radius r increases. When radius r is equal to $2t$, $E_{cluster}$ suddenly increases as mentioned before. Thus, E_{node} also suddenly increases. When radius r becomes more than $2t$ ($r > 2t$), the rate at which $E_{cluster}$ increases becomes small. Since the number of sensor nodes in a cluster keeps increasing, E_{node} once decreases. However, as radius r further increases, $E_{all_m \rightarrow h}$ and E_{head1} , which are proportional

to the number of cluster members become more influential on $E_{cluster}$. Therefore, E_{node} begins to increase again. Although we observe the minimum of E_{node} around this point, for example, $r = 205$ for $t = 50$ in Fig. 16, the radius is not feasible for the limited transmission distance of radio signals. For example, in Zigbee specifications [17], which adopts the IEEE 802.15.4 standard, the transmission range is not more than 100 meters.

In Figs. 17 through 19, we depict the transition of radius r_{opt} which minimizes E_{node} against distance t . Curves correspond to the cases that the maximum cluster radius r_{max} are 40, 80 and 100 meters and the case without limitation. Radius r has an additional limitation r_{lim} due to our analytical model. r_{lim} is defined as the boundary of conditions Fig.8 (ii) and Fig. 8 (iii), i.e., $r_{lim} = t + \sqrt{2W^2 - t^2}$. Figure 17 shows that, when $35 \leq t$ holds, radius r_{opt} is the radius which minimizes S , that is, r which minimizes $W^2 - t^2 - rt - r^2$ from Eq. (62). On the other hand, when $0 \leq t \leq 35$ holds, radius r_{opt} becomes larger than 140. This is because that radius r which minimizes $W^2 - t^2 - rt - r^2$ exceeds $2t$. In this case, the model of surface S changes from Fig. 7 (a) to Fig. 7 (b). E_{node} is also minimized at $r = 2t$, where the surface S increased suddenly, that E_{node} takes local minimum. Figs. 18 and 19 show the similar transitions. The behavior at both ends of the graph is same as in Fig. 17. However, they have differences in the intermediates, where r_{opt} becomes 75 m.

6 Simulation Experiments

We evaluated the effectiveness of our method through simulation experiments. We considered sensor networks which have a monitoring region with radius W of 100, 200, and 400. The density ρ of sensor nodes is fixed at 0.005. Then, the number of sensor nodes becomes 157, 628, and 2513 for each W . We assume that a sensor node has the limited transmission range of radio signals M_t . We set M_t at 50, 100, and 150. The maximum cluster radius r_{max} are set at 80 % of M_t . For the comparison purpose, results of fixed cluster radius are also obtained. As a fixed radius, we choose 20, 40, 80, and 120. Each sensor generates an 800-bits data every round. The message size of clustering information was set at 60 bits with a header of 120 bits. All sensor nodes had the same initial residual energy of 0.5 J.

In the following figures, Figs. 20 through 22, we depict transitions of the cumulative amount of data received at the base station and the total amount of energy consumed in each round against

the number of rounds. When sensor nodes begin to die due to depletion of battery or a tree cannot be built due to death of intermediate sensor nodes, a slope of a line becomes gentle in figures of the cumulative amount of data. The total amount of energy takes into account all of energy consumed in all four phases in our method proposed in Section 4. Figures 20, 21, and 22 correspond to cases of $W = 100, 200, \text{ and } 400$, respectively.

In figures on the right column of Figs. 20, 21, and 22, it is clearly shown that our method can reduce the total amount of energy consumed in a round. When the maximum transmission range M_t is small, a scheme with a fixed radius of $R = 20$ outperforms the others as depicted in Figs. 20(a), 21(a), and 22(a). The reason is that our multihop routing algorithm fails in establishing a tree when a cluster radius is large in comparison with the maximum transmission range. Since hearing advertisements of candidacy of others, a sensor node abandons its candidacy in our method. Cluster heads are apart from each other by at least cluster radius R . In multihop routing, the next-hop node is chosen among cluster-heads within the maximum range of radio signals, M_t . When R is close to M_t , the possibility that a cluster-head can find another cluster-head becomes small. Consequently, the cluster becomes isolated and sensor data cannot be gathered from the cluster. On the contrary, when the maximum transmission range M_t is 150, a scheme with a fixed radius of $R = 20$ becomes inferior to others as shown in Figs. 20(e), 21(e), and 22(e). When a cluster radius is small, the number of clusters becomes large. Since independently of cluster radius R , each cluster-head consumes the same amount of energy in advertising its level to the maximum transmission range of radio signals, the total amount of energy consumed in such advertisement becomes large with a small fixed radius. The effect becomes more influential when the maximum transmission range is large. When we compare results among different radii of monitoring regions, we can see that the fixed radius that leads to the best performance in terms of the amount of data received at the base station changes. Therefore, when we employ a clustering method with a fixed cluster radius, we have to carefully choose a radius in accordance with the maximum transmission range M_t and the size of the monitoring region W . On the contrary, although our protocol does not attain the best performance among alternatives, it can adapt conditions of sensor networks. We should note here that the performance degradation of our method with small M_t can be improved by introducing more sophisticated multihop routing protocol.

7 Conclusion

In this thesis, we first propose a distributed clustering method for energy-efficient data gathering in sensor networks. Next we established an analytical model of energy consumption in cluster-based data gathering with multihop communications among cluster-heads. Based on analytical results, we considered a self-organizing clustering method where each cluster-head determined its cluster radius based on the distance to the base station and other conditions of a sensor network. Through several simulation experiments, we showed that our method consumed less energy than methods with a fixed radius in sensor networks with radius of 100, 200, and 400 m. In addition, we also showed that the cluster radius for the best performance differed among conditions and our method was adaptive.

Several issues still remain to be solved. As we pointed out, our method cannot attain the best performance in spite that the total amount of consumed energy is the least, due to our poor tentative multihop routing protocol. We should consider another routing protocol that makes use of the benefit of energy-efficiency of our method.

Acknowledgements

I wish to express my gratitude to my supervisor, Prof. Masayuki Murata of Osaka University, for his extensive help and continuous support through my studies and preparation of this thesis.

I also wish to express my sincere appreciation to Prof. Makoto Imase of Osaka University, for his suggestions and comments.

I am most grateful to Associate Professor Naoki Wakamiya of Osaka University, for his appropriate guidance, hearty encouragement, and invaluable firsthand advice. All works of this thesis would not have been possible without his support.

I am indebted to Dr. Kenji Leibnitz for helpful suggestions and comments. I am also indebted to him for reading the entire text in its original form.

Finally, I heartily thank my friends and colleagues in the Department of Information Networking, Graduate School of Information Science and Technology of Osaka University for their support.

References

- [1] I. F. Akyildiz, W. Su, Y. Sankarasubramaniam, and E. Cyirci, "Wireless sensor networks: a survey," *Computer Networks*, pp. 393–422, August 2002.
- [2] W. R. Heinzelman, A. Chandrakasan, and H. Balakrishnan, "Energy-efficient communication protocol for wireless microsensor networks," in *Proceedings of the 33rd Annual Hawaii International Conference on System Sciences (HICSS)*, pp. 3005–3014, January 2000.
- [3] W. R. Heinzelman, A. P. Chandrakasan, and H. Balakrishnan, "An application-specific protocol architecture for wireless microsensor networks," *IEEE Transactions on Wireless Communications*, pp. 660–670, October 2002.
- [4] K. Dasgupta, K. Kalpakis, and P. Namjoshi, "An efficient clustering-based heuristic for data gathering and aggregation in sensor networks," in *Proceedings of the IEEE Wireless Communications and Networking Conference*, pp. 1948–1953, March 2003.
- [5] O. Younis and S. Fahmy, "Distributed clustering in ad-hoc sensor networks: A hybrid, energy-efficient approach," in *Proceedings of the 23rd Conference of the IEEE Communications Society*, pp. 629–640, March 2004.
- [6] E. Bonabeau, G. Theraulaz, and M. Dorigo, *Swarm Intelligence: From Natural to Artificial Systems*. New York : Oxford University Press, October 1999.
- [7] N. Labroche, N. Monmarché, and G. Venturini, "A new clustering algorithm based on the chemical recognition system of ants," in *Proceedings of the 15th European Conference on Artificial Intelligence*, pp. 345–349, July 2002.
- [8] A. E. Langham and P. W. Grant, "Using competing ant colonies to solve k-way partitioning problems with foraging and raiding strategies," in *Proceedings of the 5th European Conference on Artificial Life*, September 1999.
- [9] J. Kamimura, N. Wakamiya, and M. Murata, "Energy-efficient clustering method for data gathering in sensor networks," in *First Workshop on Broadband Advanced Sensor Networks*, October 2004.

- [10] A. Nasipuri and K. Li, "A directionality based location discovery scheme for wireless sensor networks," in *Proceedings of the International Conference on Mobile Computing and Networking/The first ACM international workshop on Wireless Sensor Networks and Applications*, pp. 105–111, September 2002.
- [11] R. Yamaoka, "The communication and community of ants," *NATURE INTERFACE*, no. 6, pp. 58–61, 2001.
- [12] R. Yamaoka, "How do ants recognize their nestmates?," *Quarterly Journal Biohistory*, no. 23, 1999.
- [13] K. Leibnitz, N. Wakamiya, and M. Murata, "Analytical evaluation of the transmission range in clustered sensor networks," *submitted to 19th International Teletraffic Congress (ITC-19)*, (Beijing, China), August 2005.
- [14] D. L. Hall and S. A. H. McMullen, *Mathematical Techniques in Multisensor Data Fusion*. Artech House, March 2004.
- [15] R. C. Shah and J. M. Rabaey, "Energy aware routing for low energy ad hoc sensor networks," in *Proceedings of the IEEE Wireless Communications and Networking Conference (WCNC 2002)*, March 2002.
- [16] N. Wakamiya and M. Murata, "Scalable and robust scheme for data gathering in sensor networks," in *Proceedings of the First International Workshop on Biologically Inspired Approaches to Advanced Information Technology (Bio-ADIT 2004)*, vol. LNCS3141, (Lausanne), pp. 412–427, January 2004.
- [17] "Zigbee alliance." [http:// www.zigbee.org/](http://www.zigbee.org/).

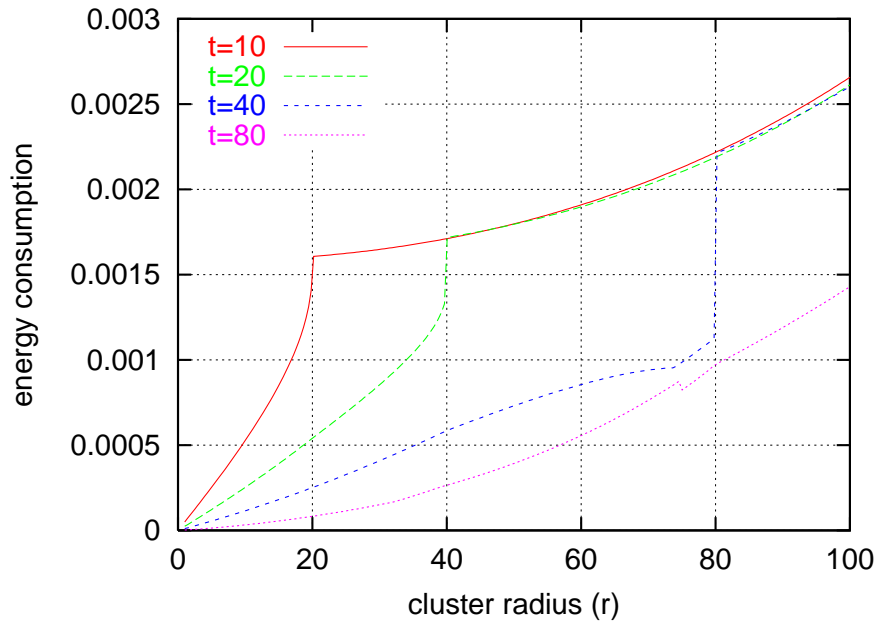


Figure 11: Transition of $E_{cluster}$ ($W = 100$)

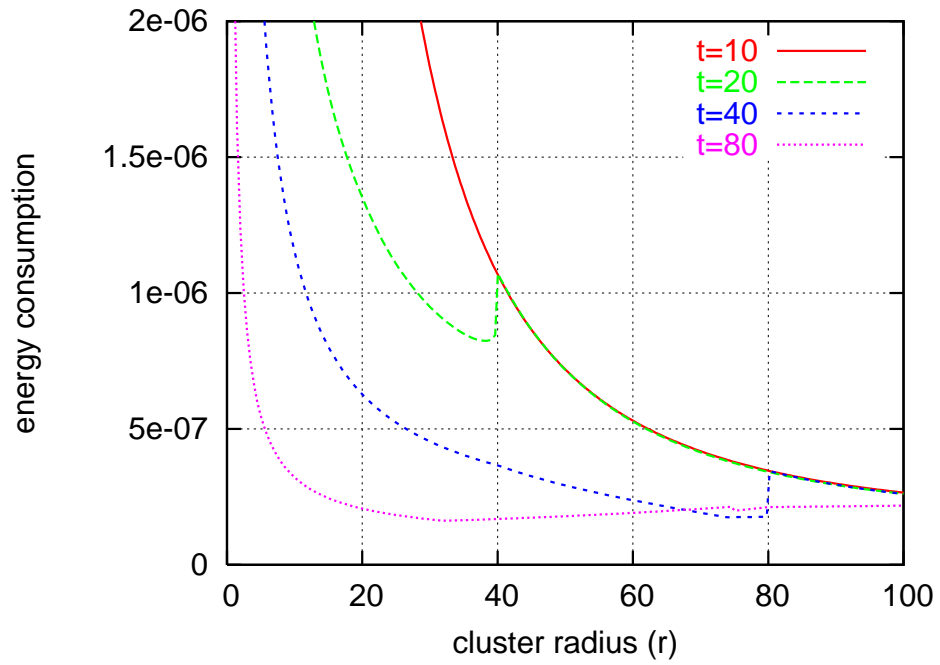


Figure 12: Transition of E_{node} ($W = 100$)

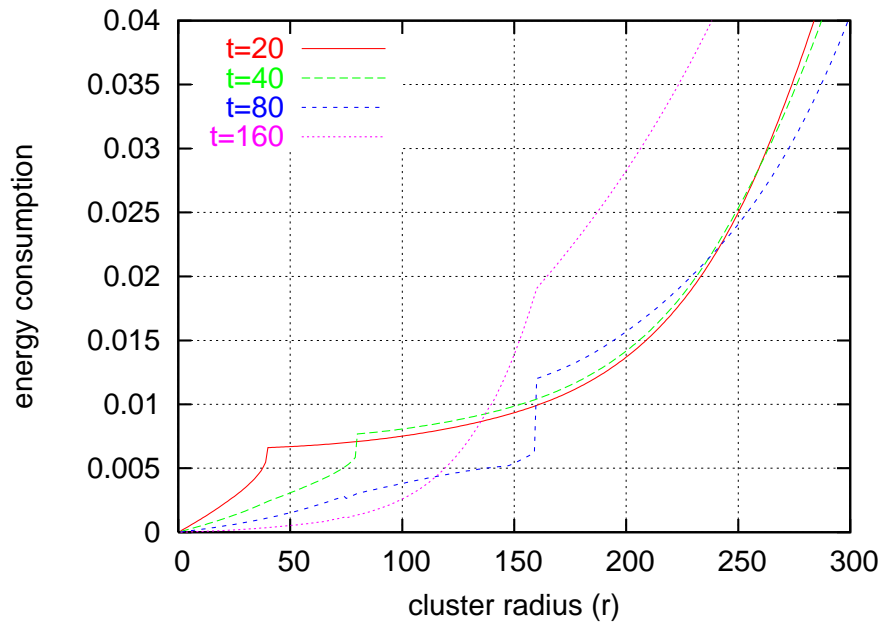


Figure 13: Transition of $E_{cluster}$ ($W = 200$)

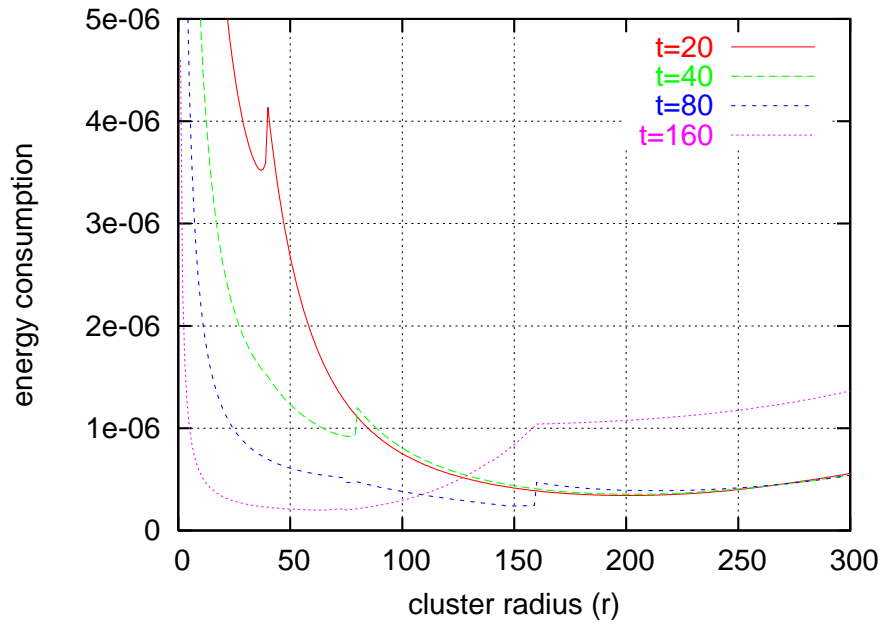


Figure 14: Transition of E_{node} ($W = 200$)

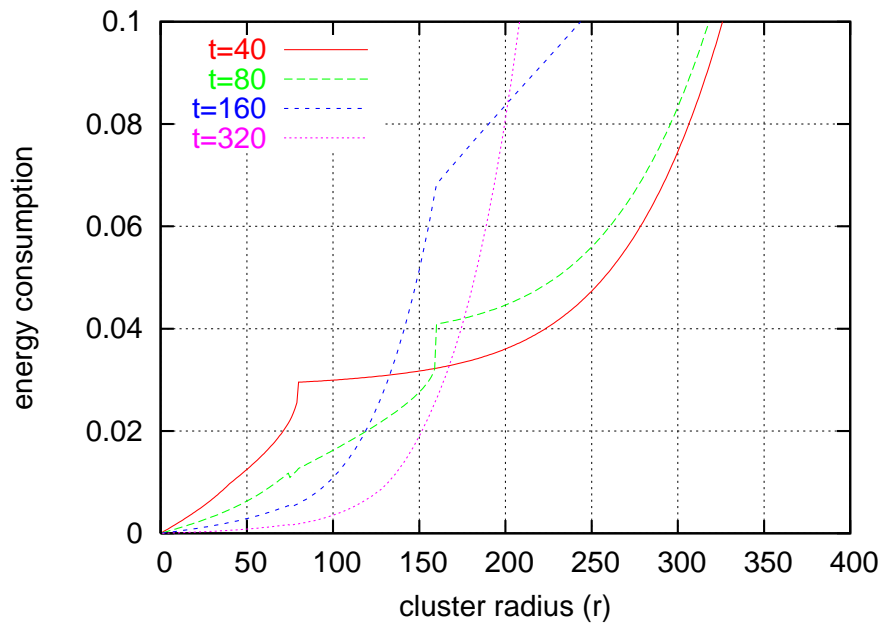


Figure 15: Transition of $E_{cluster}$ ($W = 400$)

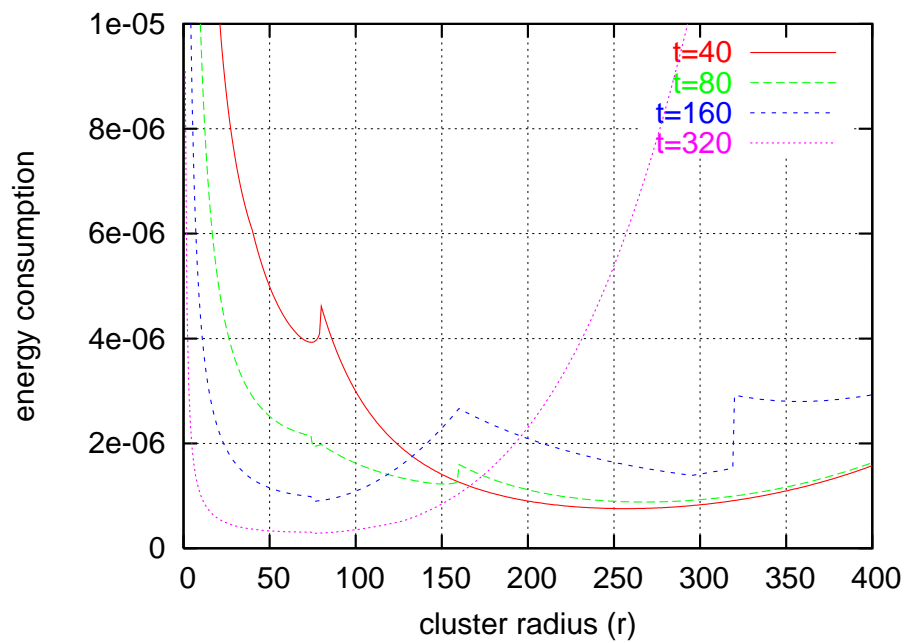


Figure 16: Transition of E_{node} ($W = 400$)

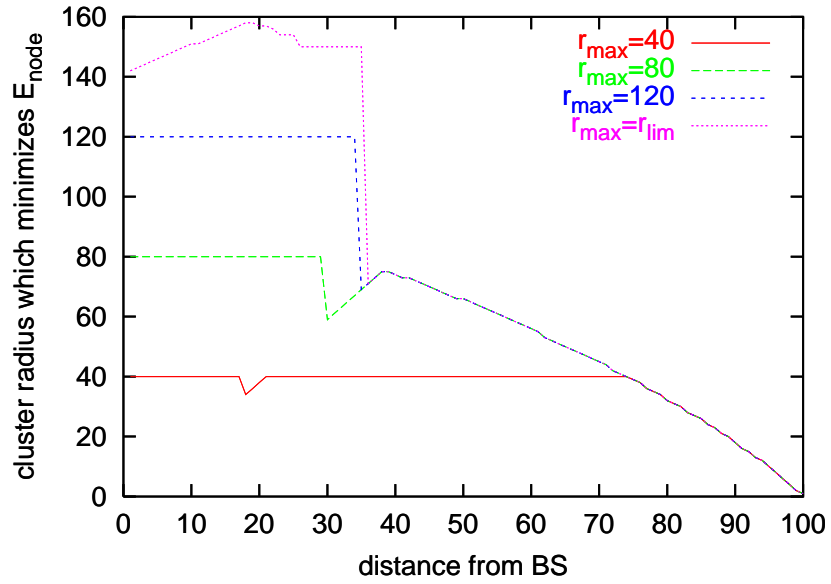


Figure 17: Transition of r_{opt} ($W = 100$)

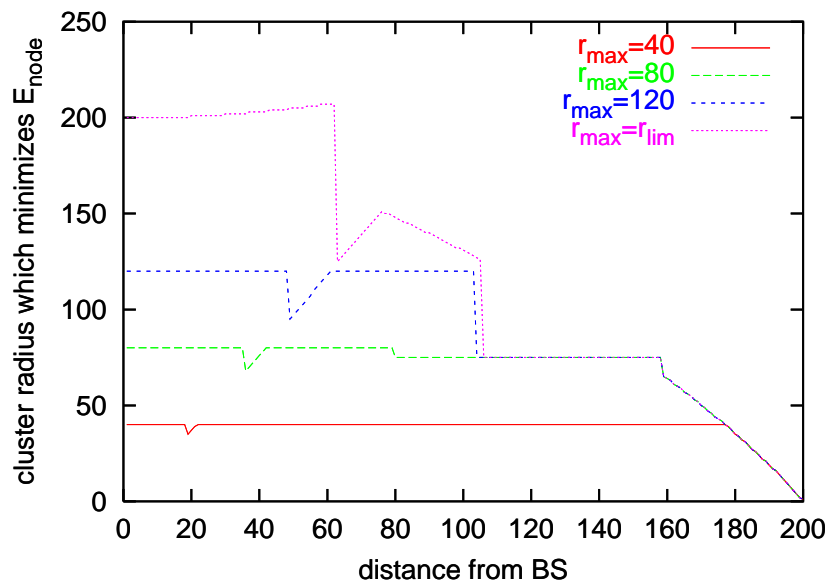


Figure 18: Transition of r_{opt} ($W = 200$)

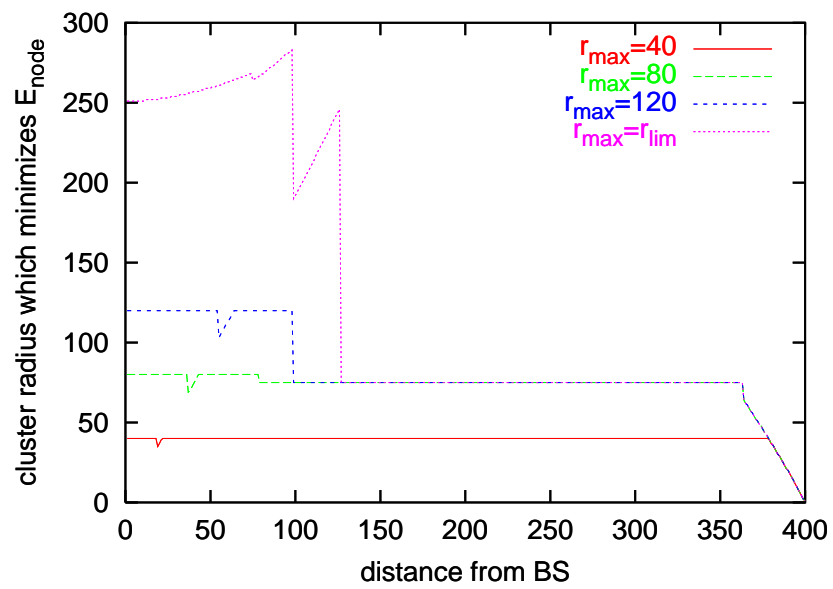
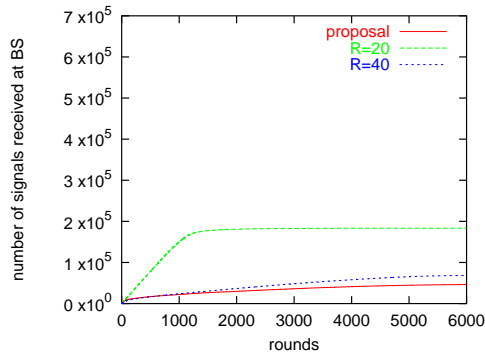
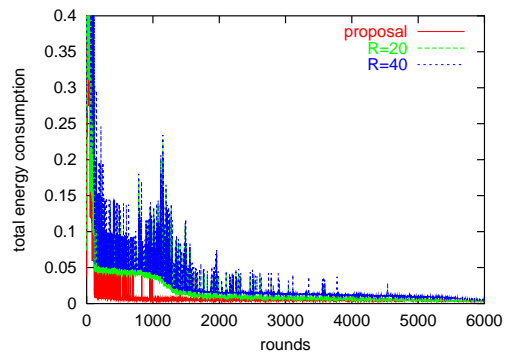


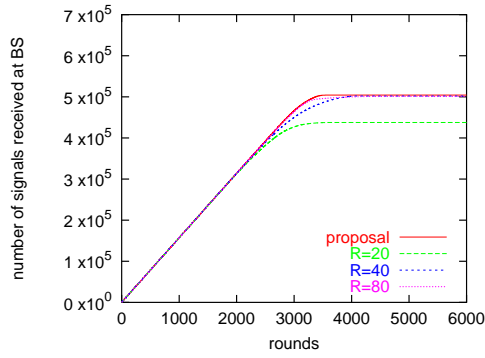
Figure 19: Transition of r_{opt} ($W = 400$)



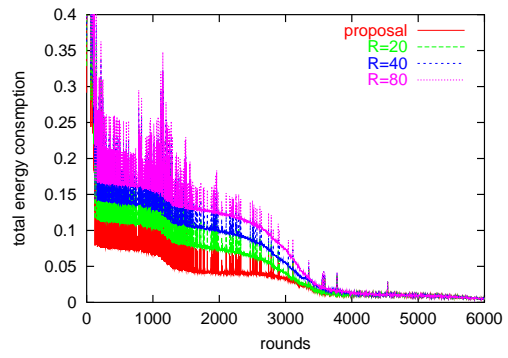
(a) Cumulative amount of received data at BS ($M_t = 50$)



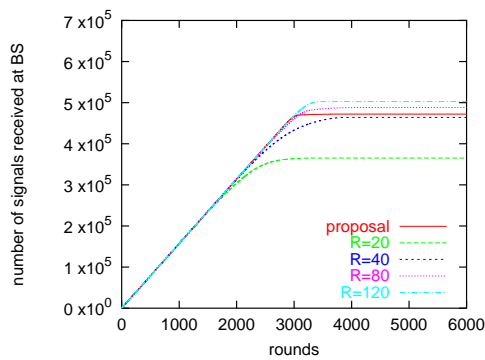
(b) Total amount consumed energy in a round ($M_t = 50$)



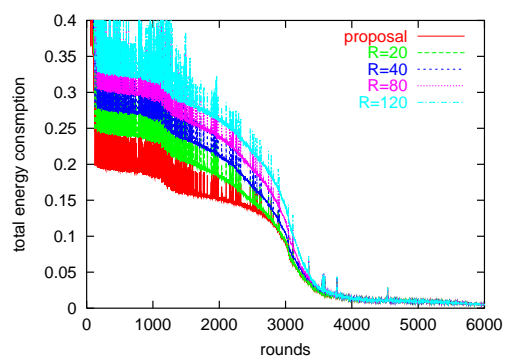
(c) Cumulative amount of received data at BS ($M_t = 100$)



(d) Total amount consumed energy in a round ($M_t = 100$)

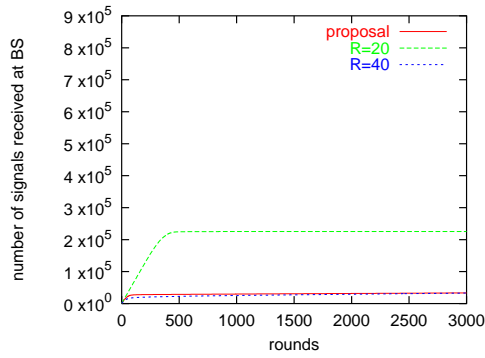


(e) Cumulative amount of received data at BS ($M_t = 150$)

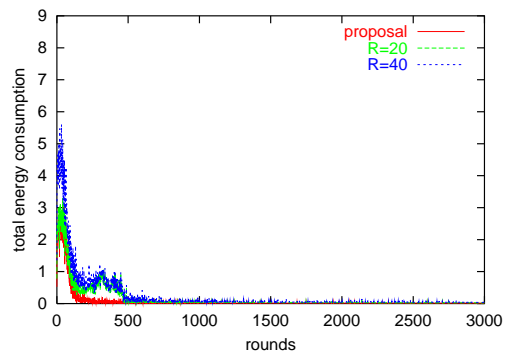


(f) Total amount consumed energy in a round ($M_t = 150$)

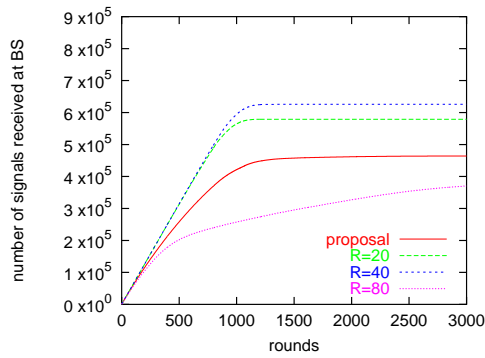
Figure 20: Cumulative amount of received data and total amount of consumed energy ($W = 100$)



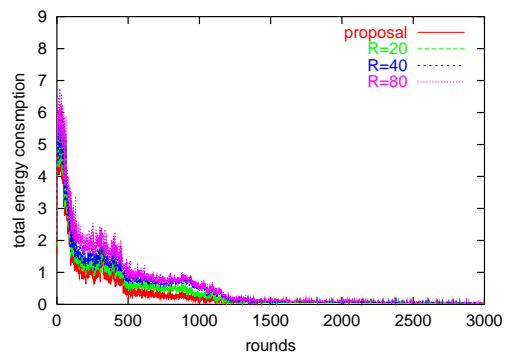
(a) Cumulative amount of received data at BS ($M_t = 50$)



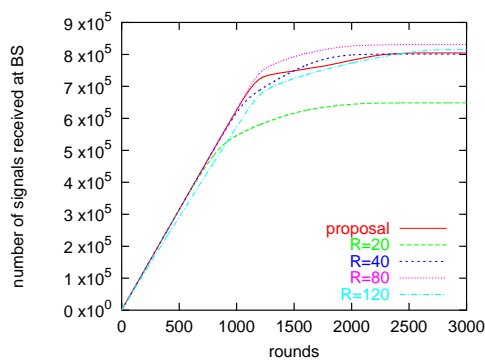
(b) Total amount consumed energy in a round ($M_t = 50$)



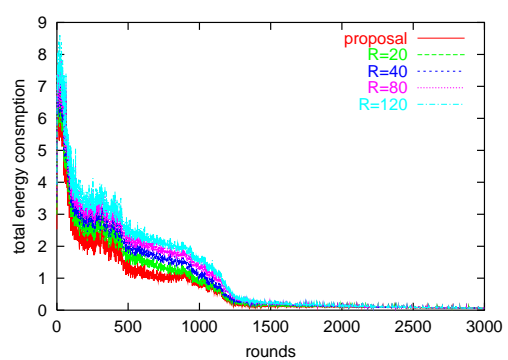
(c) Cumulative amount of received data at BS ($M_t = 100$)



(d) Total amount consumed energy in a round ($M_t = 100$)

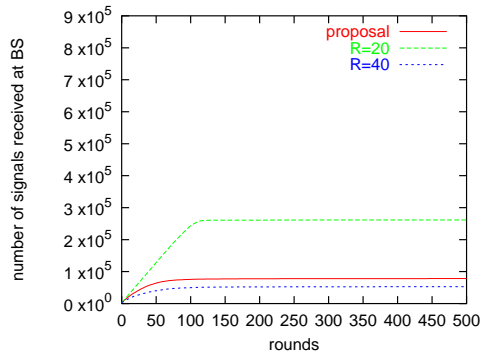


(e) Cumulative amount of received data at BS ($M_t = 150$)

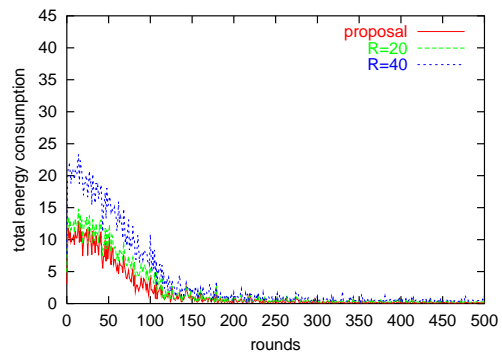


(f) Total amount consumed energy in a round ($M_t = 150$)

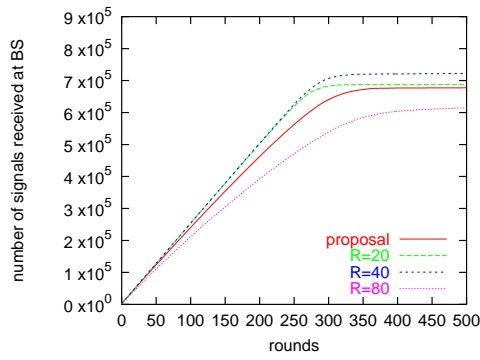
Figure 21: Cumulative amount of received data and total amount of consumed energy ($W = 200$)



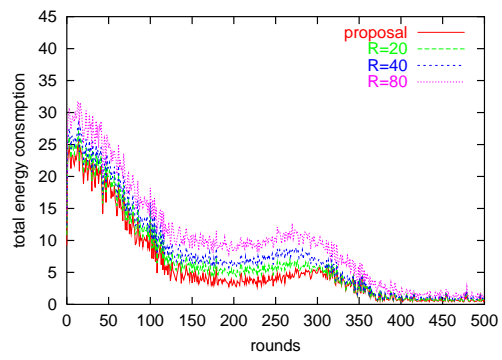
(a) Cumulative amount of received data at BS ($M_t = 50$)



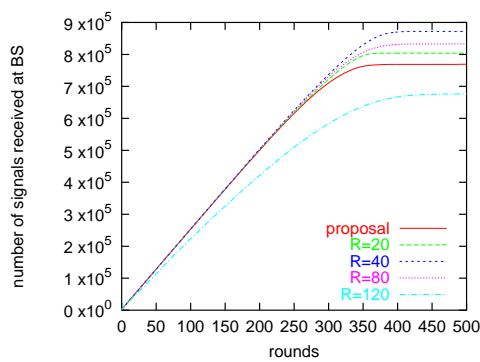
(b) Total amount consumed energy in a round ($M_t = 50$)



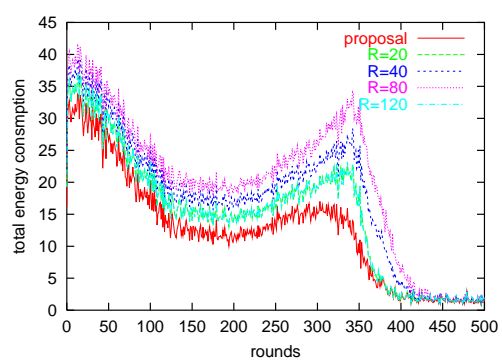
(c) Cumulative amount of received data at BS ($M_t = 100$)



(d) Total amount consumed energy in a round ($M_t = 100$)



(e) Cumulative amount of received data at BS ($M_t = 150$)



(f) Total amount consumed energy in a round ($M_t = 150$)

Figure 22: Cumulative amount of received data and total amount of consumed energy ($W = 400$)